Determination of cyclic filling length in gob-side entry retained with roadside filling and its application

Zizheng Zhang (1010096@hnust.edu.cn)
Hunan University of Science and Technology https://orcid.org/0000-0001-8764-9635
Jianbiao Bai
China University of Mining and Technology
Xianyang Yu
Hunan University of Science and Technology
Weijian Yu
Hunan University of Science and Technology
Min Deng
Hunan University of Science and Technology
Jinlin Xin
Hunan University of Science and Technology

Research

Keywords: gob-side entry retained, roadside filling area, cyclic filling length, unsupported roof length, stress difference method

Posted Date: November 17th, 2020

DOI: https://doi.org/10.21203/rs.3.rs-104890/v1

Determination of cyclic filling length in gob-side entry retained with roadside filling and its application

Zizheng Zhang[1*], Jianbiao Bai[2], Xianyang Yu[1], Weijian Yu[3], Min Deng[3] and Jinlin Xin[3]

[1] *Key Laboratory of Coal Mine Gas and Roof Disaster Prevention and Control, Hunan University of Science and Technology, Xiangtan, Hunan 411201, China;*

[2] *National Key Laboratory of Coal Resources and Safe Mining, China University of Mining and Technology, Xuzhou 221116, China;*

[3] *School of Resources, Environment and Safety Engineering, Hunan University of Science and Technology, Xiangtan, Hunan 411201, China;*

Abstract Gob-side entry retained with roadside filling (GER-RF) plays a key role in achieving coal mining without pillar and improving the coal resource recovery rate. Since there are few reports on the cyclic filling length of GER-RF, a method based on the stress difference method is proposed to determine the cyclic filling length of GER-RF. Firstly, a stability analysis mechanics model of the immediate roof above roadside filling area in GER was established, then the relationship between the roof stress distribution and the unsupported roof length was obtained by the stress difference method. According to the roof stability above roadside filling area based on the relationship between the roof stress and its tensile strength, the maximum unsupported roof length and rational cyclic filling length of GER-RF. Combined with the geological conditions of the 1103 thin coal seam working face of Heilong Coal Mine and the geological conditions of the 1301 thick coal seam working face of Licun Coal Mine, this suggested method was applied to determine that the rational cyclic filling lengths of GER-RF were 2.4 m and 3.2 m, respectively. Field trial tests show that the suggested method can effectively control the surrounding rock deformation along with rational road-in support and roadside support, and improve the filling and construction speed.

Key words gob-side entry retained, roadside filling area, cyclic filling length, unsupported roof length, stress difference method

1. Introduction

1.1 Literature review of GER-RF

In recent years, gob side entry retained (GER) without coal pillar mining technology has its advantages. These advantages include alleviating the contradiction of excavation replacement, improving coal recovery rate, and realizing working face Y-type ventilation, and solving corner gas accumulation. GER has been developed into one of the green, safe, and efficient mining technologies for coal resources (Kang et al. 2010; Han et al. 2019; Zhang et al. 2015; Yang et al. 2020). Since the 1950s, China and other major coal producing countries have carried out many industrial tests of GER. Ning proposed a GER case with a “coal-backfill-gangue” support system in the thin coal seam (1.3 m) of Binhu Coal Mine (Ning et al. 2018). Zhang proposed a GER case with thick and hard roof in the medium-thick coal seam (3.0 m) of Xinchao Coal Mine (Zhang et al. 2018). Luan proposed a GER case with thick and hard roof in the thin coal seam (1.25 m) of Dongtan Coal Mine (Luan et al. 2018). Tian proposed a GER case with soft roof, floor, and seam in the thin coal seam (1.3 m) of Heilong Coal Mine (Tian et al. 2020). Wang proposed a no-pillar mining technique with automatically formed GER in the thick coal seam (4.11 m) of Ningtiaota Coal Mine (Wang et al. 2018). Huang proposed a GER case using concrete-filled steel tubular column as roadside supporting in the thin coal seam (1.15 m) (Huang et al. 2018). Su proposed a GER case in

fully-mechanized longwall with top-coal caving in the thick coal seam (6.3 m) of Yuwu Coal Mine (Su et al. 2015). Zhang proposed a GER case with supercritical retained entry width in the thick coal seam (4.0 m) of Liujiazhuang Coal Mine (Zhang et al. 2019). Zhang proposed a GER case in the medium-thick coal seam (2.8 m) of Xinyuan Coal Mine (Zhang et al. 2020). Therefore, GER engineering applications have developed from thin coal seam and medium-thick coal seam to thick coal seam mining. The GER technology with roadside filling is one of the widely used GER technologies. When the roadside filling is carried out, the roadside filling body generally lags behind the end support of the working face. The filling area near the roadway is often in the state of no support or simple temporary support, that is, the support strength of the area to be filled is low, which is called "lagging unsupported roof" (see Fig.1). Zhang and Zheng firstly proposed that roof stability in the filling area is one of the key factors for the success of GER (Zhang et al. 2018; Zhang et al. 2020; Zhang et al. 2012). The length of the lagging unsupported roof in GER-RF is mainly composed of the cyclic filling length and the width of the pedestrian passage behind the support. The width of the pedestrian passage is generally 0.8 m. Therefore, the cyclic filling length in GER-RF is the bottleneck to improve the construction speed of the roadside filling body.

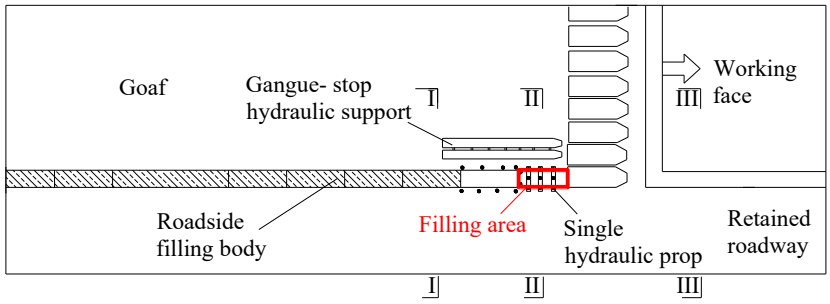

(a) plan view of GER-RF

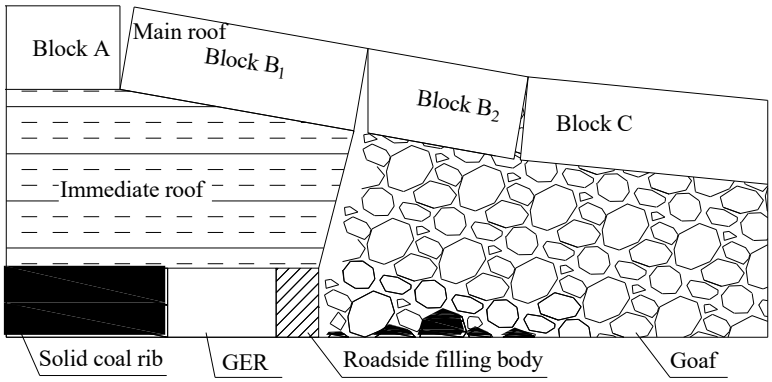

(b) section view of I-I

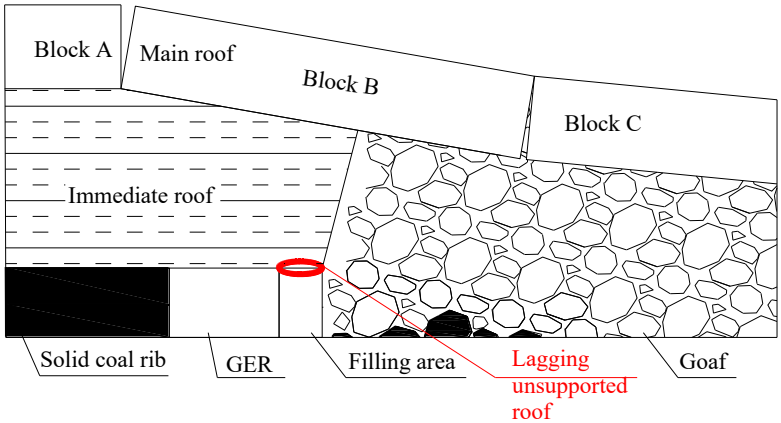

(c) section view of II-II

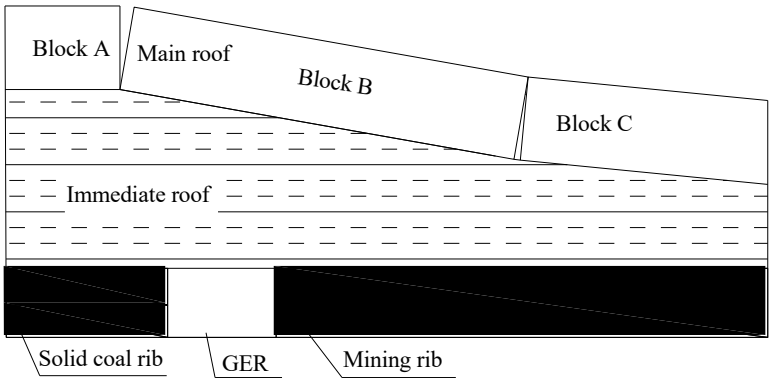

(d) section view of III-III

Fig. 1 Sketch of lagging unsupported roof in GER-RF

1.2 Literature review of the cyclic filling length in GER-RF

At present, the daily mining length of high-efficiency fully mechanized mining working face in China is usually more than 4.8 m. Due to the early strength performance, solidification time, and resistance increasing speed of existing filling materials (Kang et al. 2010; Han et al. 2019; Zhang et al. 2018; Luan et al. 2018; Wang et al. 2018), the roadside filling body may not be constructed in time or the built roadside filling body cannot reach the designed support resistance in time, the length of the lagging unsupported roof will increase. When the length of the lagging unsupported roof is too large, the lower part of the immediate roof may lose stability under the action of tensile stress (Zhang et al. 2018). Therefore, how to determine the rational cyclic filling length in GER-RF is very important to match the daily mining length of high-efficiency fully mechanized mining working face. However, the cyclic filling length was manually determined previous, and there are no published reports at home and abroad on the determination method and theory of the cyclic filling length in GER-RF.

This paper presents a method to determine the length of the lagging unsupported roof and the cyclic filling length in GER-RF. Firstly, the mechanical model of the immediate roof stability analysis above the roadside filling area in GER-RF is established. The relationship between the stress distribution of immediate roof above the roadside filling area and the length of the lagging unsupported roof is calculated by means of the stress difference method. Then, the stability of the immediate roof above roadside filling area in GER-RF is determined according to the comparison between the immediate roof stress and ultimate tensile strength. On the basis of this, the reasonable length of the lagging unsupported roof and the cyclic filling length in GER-RF are determined. Finally, the method is carried out in two different thickness coal seams (thin coal seam, thick coal seam) with high water materials roadside filling and GER engineering practice.

2. Mechanical model of immediate roof stability analysis above roadside filling area in GER-RF

It is very important to determine the length of the lagging unsupported roof during the construction of the roadside filling body. When the length of the lagging unsupported roof is too large, the roof above the roadside filling area is prone to collapse. When the length of the lagging unsupported roof is too small, the filling cycle times are more and the utilization rate of the filling body support is low. Under this condition, the construction speed of the roadside filling body is affect and the working efficiency of the high-efficiency fully mechanized mining working face is limited. The existing study show that the lower strata of the immediate roof are in the range of tensile stress, and with the increase of the rotation subsidence angle of the main roof (the process of increasing the support resistance of the roadside filling body), the scope of the tensile stress gradually decreases (Zhang et al. 2018). It can be seen that the roof of the area to be filled is mainly the tensile failure of the shallow immediate roof. The temporary support of the area to be filled and its surrounding is mainly to prevent the collapse of the immediate roof in the

lagging unsupported roof area to be filled. In reality, the immediate roof above the roadside filling area in GER-RF is affected by the abutment pressure in front of the hydraulic support of the working face. The subsidence of the immediate roof gradually increases until the built roadside filling body starts to support the immediate roof. As a result, the cumulative damage of the immediate roof rock increases gradually. Therefore, the immediate roof of the area to be filled is the key to control surrounding rock during the filling period of GER-RF.

A large area of suspended roof will form at the end of the working face before the filling body is built along the goaf. The immediate roof in the area to be filled may be in the stage of no support or low support strength, as shown in Fig. 2a. The roof is supported by the coal wall in front of the working face, the hydraulic support at the end, and the newly built backfill. Therefore, a mechanical model of immediate roof stability analysis above the roadside filling area in GER-RF is established as shown in Fig. 2b. The main assumptions of the model are as follows :(1) the immediate roof can be regarded as a rock beam with the same support stress as the overburden pressure, roadside support force, end hydraulic support force, and abutment pressure in a certain range in front of the working face; (2) the pressure load above the immediate roof (including the weight of the immediate roof) is q, and below the immediate roof are the support loads provided or passively generated by the coal wall support section, the end hydraulic support section and the roadside filling body section of the retaining roadway, respectively, which are q_1, q_2 and q_4, the length of each corresponding segment is L_1, L_2, and L_4 respectively; (3) in the model, the sum of L_3 and L_4 is calculated according to the periodic weighting length of the main roof. (4) L_2 is the total length of the top beam of the hydraulic support; (5) L_1 is selected according to the position of the peak abutment pressure in front of the coal wall; (6) the main roof is assumed to be rigidity.

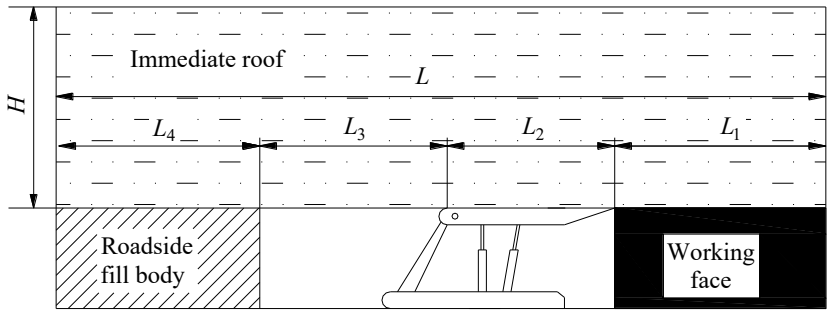

(a) Section of GER-BB along the strike direction.

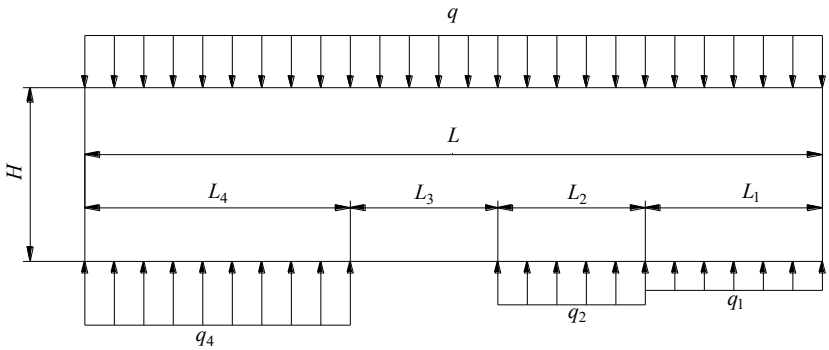

(b) Immediate roof mechanical model in GER-RF along the strike direction.

Fig.2 Mechanical model of immediate roof stability analysis above roadside filling area in GER-RF

3. Immediate roof stress component solution of roadside filling area based on the stress difference method

Difference method is an approximate numerical solution of differential equations, including stress difference method and displacement difference method. Specifically, the difference method is to replace the differential equation with a finite difference, and the derivative with a finite difference quotient, so that the basic equation and boundary condition (generally differential equation) are approximately expressed by the difference equation

(algebraic equation), and the problem of solving differential equation is changed into the problem of solving algebraic equation. In elastic mechanics, the difference method and the variational method are used to solve plane problems.

Take the 5 m thick immediate roof as an example, when L_3 is 5.0 m, the periodic weighting length (L_3+ L_4) is 15 m, and the top beam length of the end bracket (L_2) is 5 m. L_1 is assumed to be 10 m, namely, the total length (L) is 30 m. The difference grid of the immediate roof is divided along the roadway strike and vertical direction, with each grid length of 0.5 m, as shown in Fig. 3. The boundary load of the model is applied. Then the stress difference method is used to solve the stress component of the immediate roof of the retained roadway.

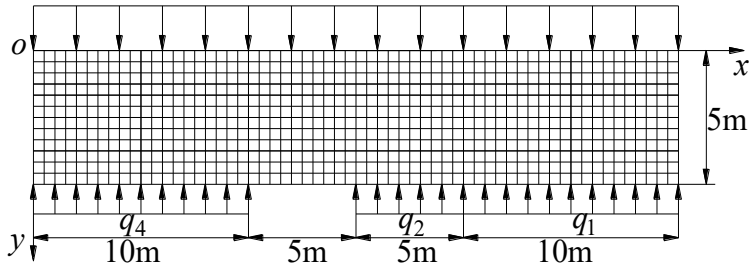

Fig.3. Finite difference elements of the immediate roof in GER-RF

First of all, q_1 and q_4 are determined by the following formula according to the mechanical equilibrium.

$$\begin{cases} q_0 L = q_1 L_1 + q_2 L_2 + q_4 L_4 \\ \frac{1}{2} q_0 L^2 = \frac{1}{2} q_1 L_1^{\,2} + \frac{1}{2} q_2 \left[\left(L_1 + L_2 \right)^2 - L_1^{\,2} \right] + \frac{1}{2} q_4 \left[L^2 - \left(L_1 + L_2 + L_3 \right)^2 \right] \end{cases} \quad (1)$$

Secondly, the stress difference method and software programming are used to solve the stress function of the immediate roof along the goaf (Bai et al. 2011; Yan et al. 2020). Part of the model is taken for solution explanation (as shown in Fig.4). In Fig.4, the grid width in x and y directions is equal, A and B are nodes numbered, φ is the stress function, and φ_i represents the stress value with node number i.

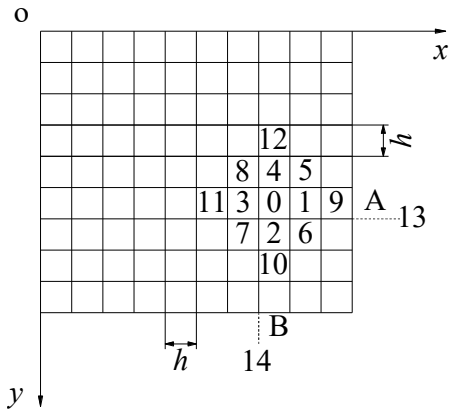

Fig.4 Schematic diagram of the stress difference method

The stress difference method is used to calculate the stress component of the immediate roof of the retained roadway (Bai et al. 2011; Yan et al. 2020):

1) Arbitrarily select A node on the boundary as the base point,

$$\varphi_A = \left(\frac{\partial \varphi}{\partial x} \right)_A = \left(\frac{\partial \varphi}{\partial y} \right)_A = 0 \quad (2)$$

Then the φ value of all nodes on the boundary and the necessary value and value of formula (3) are calculated by

the sum of the moment and surface force of the surface force, $\frac{\partial \varphi}{\partial x}$ and $\frac{\partial \varphi}{\partial y}$.

$$\begin{cases} \varphi_{13}=\varphi_9+2h\left(\dfrac{\partial \varphi}{\partial x}\right)_A \\ \varphi_{14}=\varphi_{10}+2h\left(\dfrac{\partial \varphi}{\partial y}\right)_B \end{cases} \tag{3}$$

The left side of the equation is the imaginary node outside the boundary, and the right side is the real node.

2) Formula (3) is applied to represent the φ value of each virtual node on the boundary with the φ value of the corresponding node within the boundary.

3) At node 0, the difference equation is

$$\varphi_0 - 8(\varphi_1+\varphi_2+\varphi_3+\varphi_4)+2(\varphi_5+\varphi_6+\varphi_7+\varphi_8)+(\varphi_9+\varphi_{10}+\varphi_{11}+\varphi_{12})=0 \tag{4}$$

For each node in the boundary, such a difference equation can be established and solved simultaneously, so as to find out the value of each node.

4) According to Formula (3), calculate the value of each virtual node in a row outside the boundary.

5) Calculate the stress component according to Equations (5) ~ (7).

$$(\sigma_x)_0=\left(\frac{\partial^2 \varphi}{\partial y^2}\right)_0=\frac{1}{h^2}\left[(\varphi_2+\varphi_4)-2\varphi_0\right] \tag{5}$$

$$(\sigma_y)_0=\left(\frac{\partial^2 \varphi}{\partial x^2}\right)_0=\frac{1}{h^2}\left[(\varphi_1+\varphi_3)-2\varphi_0\right] \tag{6}$$

$$(\tau_{xy})_0=\left(-\frac{\partial^2 \varphi}{\partial y^2}\right)_0=\frac{1}{h^2}\left[(\varphi_5+\varphi_7)-(\varphi_6+\varphi_8)\right] \tag{7}$$

Similarly, the stress components of other nodes can be obtained. Due to a large number of nodes, the simultaneous solution of multiple equations requires a large amount of computational work, which needs to be solved by programming software and in accordance with the above calculation steps.

4. Determination method and realization process of cyclic filling length in GER-RF

Based on the stress difference method, the method and realization process to determine the cyclic filling length in GER-RF is as follows:

1) Firstly, according to the mining and geological conditions of the retained roadway, the mechanical model of immediate roof stability analysis above roadside filling area in GER-RF was established and grid division was carried out;

2) Then, the relevant parameters required in Section 2 are selected according to the mining and geological conditions of the retained roadway and the rock mechanics parameters of surrounding rocks;

3) In view of different length of the lagging unsupported roof schemes, considering that the difference of each level of the length of the lagging unsupported roof is less than shearer cutting depth, gradually increase the length of the lagging unsupported roof, calculate and solve respectively, and obtain the corresponding maximum tensile stress;

4) The maximum tensile stress under each scheme is recorded, and the relevant maximum tensile stress is compared with the immediate roof tensile strength above roadside filling area under this scheme, so as to determine whether the maximum tensile stress under this scheme exceeds the immediate roof tensile strength, and then determine the maximum length of the lagging unsupported roof in GER-RF;

5) According to the maximum length of the lagging unsupported roof in GER-RF and the minimum width of the

pedestrian passage, determine the reasonable cyclic filling length in GER-RF.

Fig. 5 shows the realization process of determining the cyclic filling length in GER-RF based on the stress difference method.

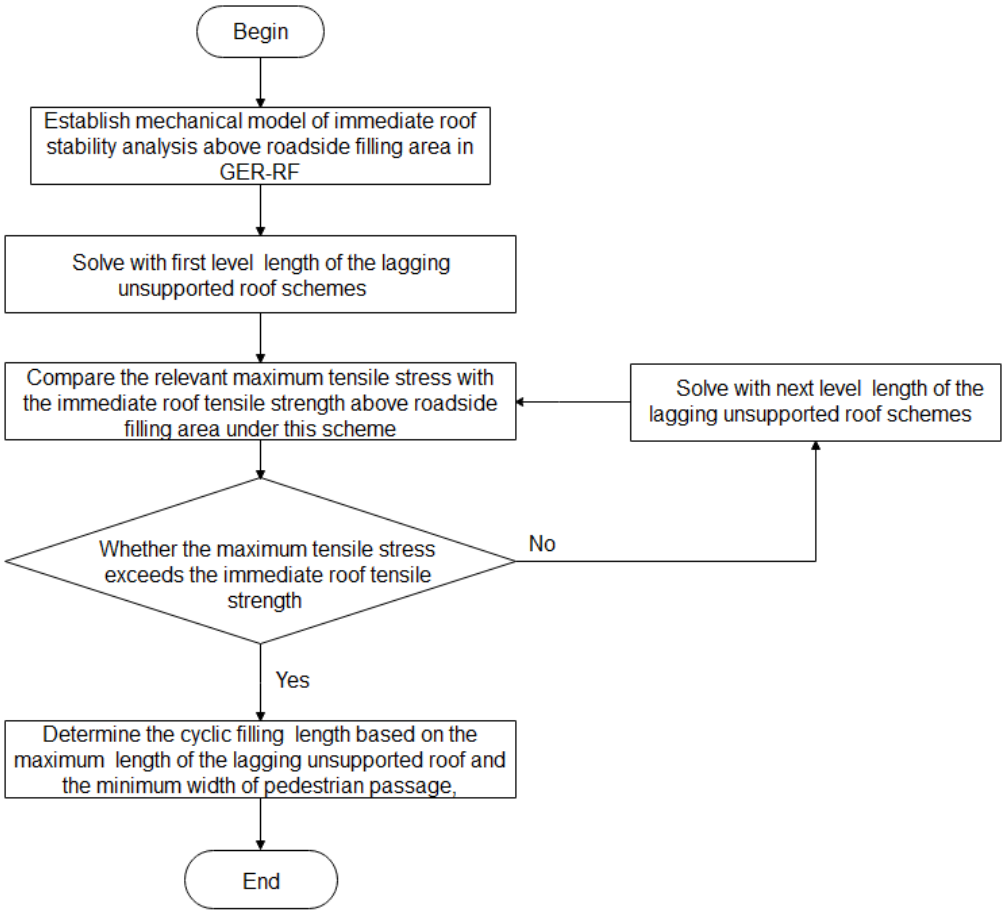

Fig.5 Calculation flow of the cyclic backfill length of GER-BB based on the stress difference method.

5. Engineering Analysis

5.1. GER of #1103 working face in Heilong Coal Mine (thin coal seam)

5.1.1. Project Overview

The #1103 working face in Heilong Coal Mine in Puxian County of Shanxi Province has an average thickness of 1.3 m and a buried depth of 210 m. The coal seam dip Angle is 0~20°, an average 10°. The coal seam contains no gangue, simple structure, and stable layer. #1103 working face as the low gas face, the self-ignition orientation of coal is classified into level II. #1103 working face mining engineering plan is shown in Fig. 6 (a), and comprehensive column chart of coal seam and roof and floor of #1103 working face is shown in Fig. 6 (b).

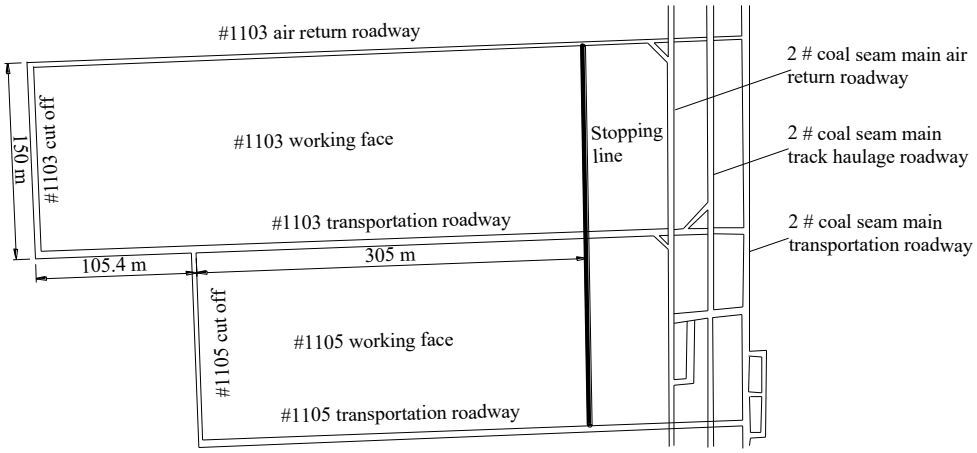

(a) Mining plan of #1103 working face.

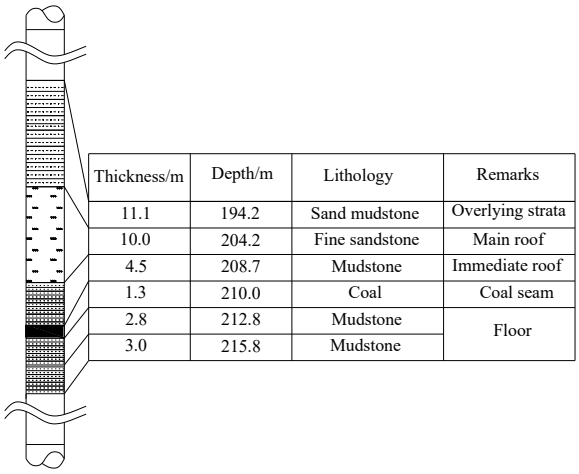

Thickness/m	Depth/m	Lithology	Remarks
11.1	194.2	Sand mudstone	Overlying strata
10.0	204.2	Fine sandstone	Main roof
4.5	208.7	Mudstone	Immediate roof
1.3	210.0	Coal	Coal seam
2.8	212.8	Mudstone	Floor
3.0	215.8	Mudstone	

(b) Comprehensive column chart of coal seam and roof and floor of #1103 working face.

Fig.6 Geological conditions of production at #1103 working face in Heilong Coal Mine.

The designed length of #1103 working face is 150 m, and the #1103 transport roadway opening is in the main transport roadway of No. 2 coal seam, with a designed length of 531.4 m. The #1103 transport roadway is used as the air-return roadway of #1105 working face after GER. The #1103 transport roadway section is a rectangular section with width × height 4.0 m × 2.3 m. It is tunneled along the roof of the coal seam and supported by rock bolts, anchor cables, and metal meshes. The roof in the roadway is supported by left-hand screw thread steel bolt of Φ18 mm × L2.0 m, the row spacing of anchor bolts is 0.9 m × 1.0 m. The pre-stressed anchor cable of Φ17.8mm × L6.3 m is used for roof support, and the row spacing between anchor cables is 2.0 m × 3.0 m. Three Φ18mm × L2.0 m deformed steel bars are arranged on both sides of the roadway, and the spacing between rows is 0.9 m × 1.0 m.

The end hydraulic support of the #1103 working face is ZT4000/14/30, the length of the top beam of the hydraulic support is 5.5 m, and the supporting strength is 0.6 MPa. The cutting depth of the coal cutter is 0.6 m, and the working face periodic weighting length of the main roof is 15m. The thickness of the immediate roof is 4.5 m, the tensile strength is 0.35 MPa, and the compressive strength is 16.1 MPa. The roadside filling body of #1103 transport roadway is constructed with high water quick-setting materials and water-cement ratio of 1.5:1, with a width of 1.2 m. In order to facilitate the construction of the roadside filling body, the minimum pedestrian width behind the end hydraulic support is 0.8 m.

At the same time, a row of Φ18.9 mm × L6.3 m anchor cables are added in the middle of the two rows of roadway roof bolts without anchor cables, and the row spacing is 2.0 m × 1.0 m. A row of Φ8 mm × L2.0 m bolts are added in the middle of the two rows of roadway rib bolts. The single hydraulic prop and type steel beam are used to

reinforce the retained roadway within the 80 m range behind the working face, and the column row spacing is 1.2 m×1.0 m.

5.1.2 Determine the cyclic filling length in GER-RF of #1103 working face

According to the above comprehensive column chart, the overburden thickness can be determined to be 14.5 m (4.5 m+10 m), and the average bulk density is 2.5 t/m^3, the load of the overburden rock layer is 0.3625 MPa. According to the above, L_1= 10 m, L_2 = 5.5 m, L_3+ L_4= 15 m. By substituting the above data into the calculation, the immediate roof horizontal stress distribution cloud map of the retained roadway with different lengths of the lagging unsupported roof is obtained, as shown in Fig. 7.

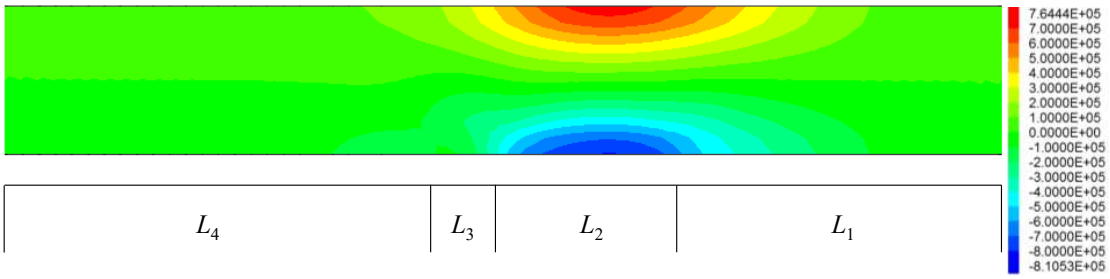

(a) Length of the lagging unsupported roof is 2.0 m.

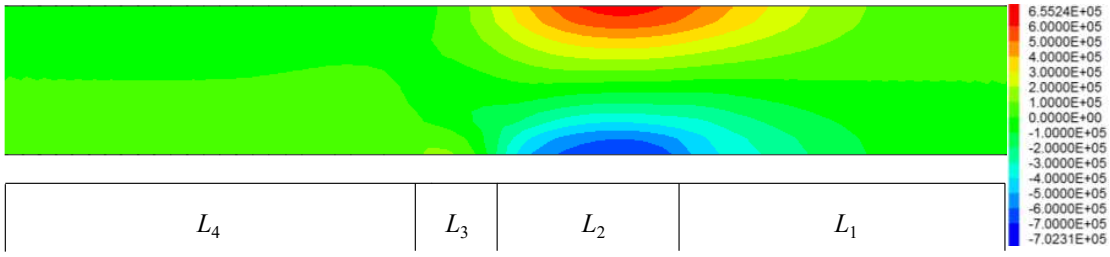

(b) Length of the lagging unsupported roof is 2.5 m.

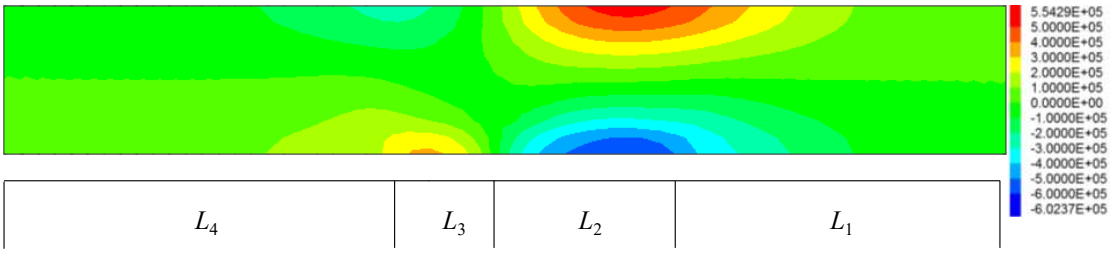

(c) Length of the lagging unsupported roof is 3.0 m.

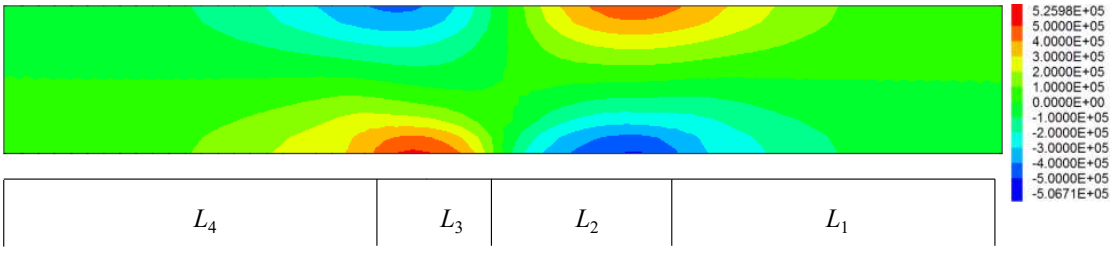

(d) Length of the lagging unsupported roof is 3.5 m.

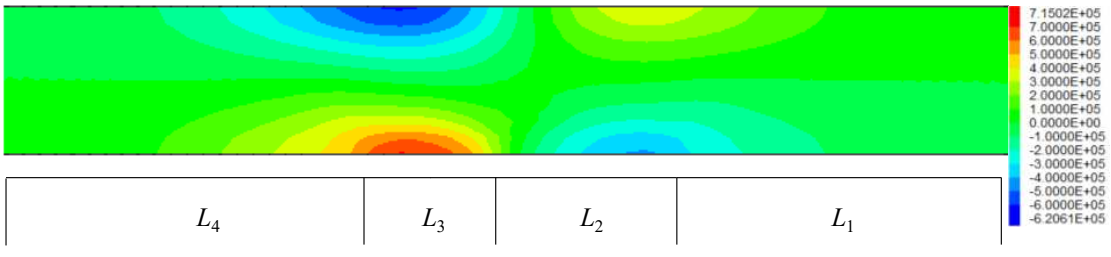

(e) Length of the lagging unsupported roof is 4.0 m.

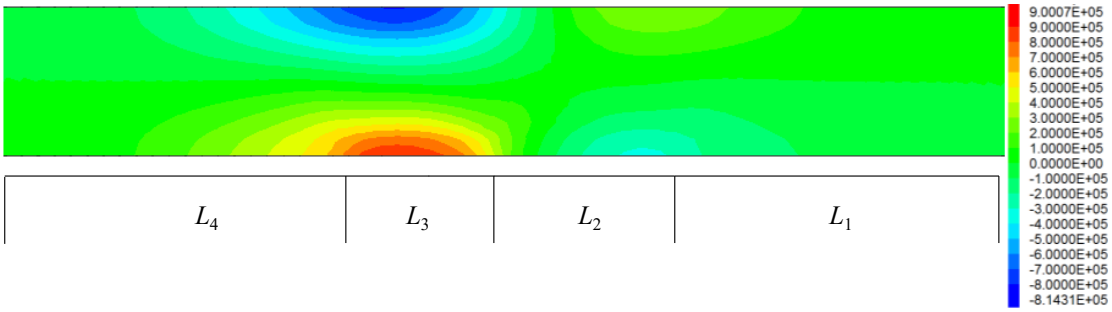

(f) Length of the lagging unsupported roof is 4.5 m.

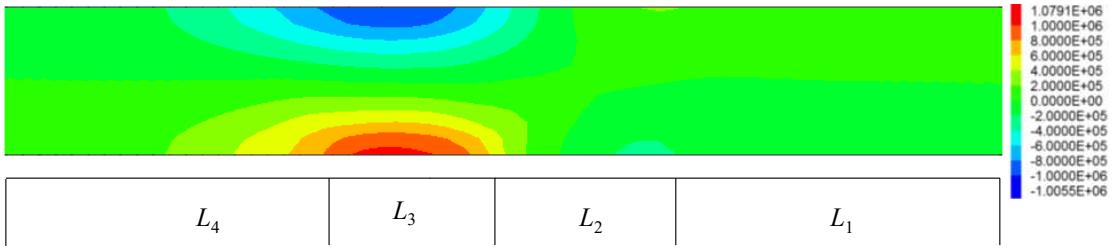

(g) Length of the lagging unsupported roof is 5.0 m.

Fig. 7 Immediate roof horizontal stress distribution cloud map of the retained roadway with different lengths of the lagging unsupported roof. (unit:Pa).

According to Fig. 7, the horizontal stress distribution of the immediate roof of the retained roadway with different length of the lagging unsupported roof is as follows:

1) When the length of the lagging unsupported roof is no more than 2.5 m, the upper immediate roof rock is subjected to the tensile stress, while the lower immediate roof rock is subjected to the compressive stress. The maximum compressive stress occurs in the middle of the immediate roof bottom boundary of the end hydraulic support section and the maximum tensile stress occurs in the middle of the immediate roof boundary of the end hydraulic support section.

2) When the length of the lagging unsupported roof is greater than 2.5 m and less than 4.5 m, the upper immediate roof rock above the unsupported area is subjected to compressive stress, and the lower immediate roof rock above the unsupported area is subjected to tensile stress. The upper immediate roof rock above end hydraulic support is subjected to compressive stress, and the lower immediate roof rock above end hydraulic support is subjected to tensile stress.

3) When the length of the lagging unsupported roof is greater than 4.5m, the upper immediate roof rock is subjected to compressive stress, and the lower immediate roof rock is subjected to tensile stress. The maximum tensile stress occurs in the middle of the lower boundary above the unsupported area and the maximum compressive stress occurs in the middle of the upper boundary above the unsupported area.

With the increase of the length of the lagging unsupported roof, the maximum tensile stress at the lower part of the immediate roof above unsupported area gradually increases, and the detailed results are shown in Table 1.

Table 1 Maximum tensile stress of the lower immediate roof in GER-RF with respect to the length of the lagging unsupported roof and cyclic filling length.

Length of the lagging unsupported roof /m	Cyclic filling length /m	Maximum tensile stress /MPa
2.0	1.2	-0.095 (in this case, compressive stress)
2.5	1.7	0.12
3.0	2.2	0.32
3.5	2.7	0.52
4.0	3.2	0.72

4.5	3.7	0.9
5.0	4.2	1.08

According to the aforementioned immediate roof tensile strength of 0.35 MPa, when the length of the lagging unsupported roof is no less than 3.5 m (cyclic filling length is no less than 2.7 m), the lower immediate roof rock above the roadside filling area is subjected to the tensile stress. Taking integer times of the coal cutter cutting depth, the rational cyclic filling length is 2.4 m.

5.1.3 Model validation and implementation effect

No caving or other instability failure occurred in the filling area during the implementation of GER-RF. This indicates that the cyclic filling length and the length of the lagging unsupported roof are appropriate and the proposed model is rational. The in-situ monitoring results show that the surrounding rock deformation of the retained roadway tends to be stable 80 m behind the #1103 working face, the maximum displacement of the roof to floor is 1429.6 mm, and the displacement of two ribs is not more than 490.1 mm.

Fig. 8 shows the implementation effect of GER-RF in Heilong Coal Mine. The above monitoring shows that the surrounding rock of the retained roadway is basically intact after GER-RF, which meets the expected requirements, and the cyclic filling length of the roadside filling body determined by the study meets the requirements for ensuring safe construction of GER-RF.

Fig. 8 GER implementation effect of #1103 working face in Heilong Coal Mine

5.2 GER of #1301 working face in Licun Coal Mine (thick coal seam)

5.2.1. Project Overview

Licun Coal Mine is located in Changzhi City, Shanxi Province, with a designed production capacity of 3.0 million tons per year. There are three coal seams in the mine, of which No.3 and No.15 coal seams are the main coal seams. No.3 coal seam is the high-gassy coal seam with outburst. #1301 working face is the first mining working face of the mine, without mining activities all around. The average coal thickness is 4.2 m, and the average dip angle is 3°, and the buried depth is 597 m ~ 561 m. Fig. 9(a) shows the excavation plan of #1301 working face. Fig. 9(b) shows the comprehensive column chart of coal seam and roof and floor of #1301 working face.

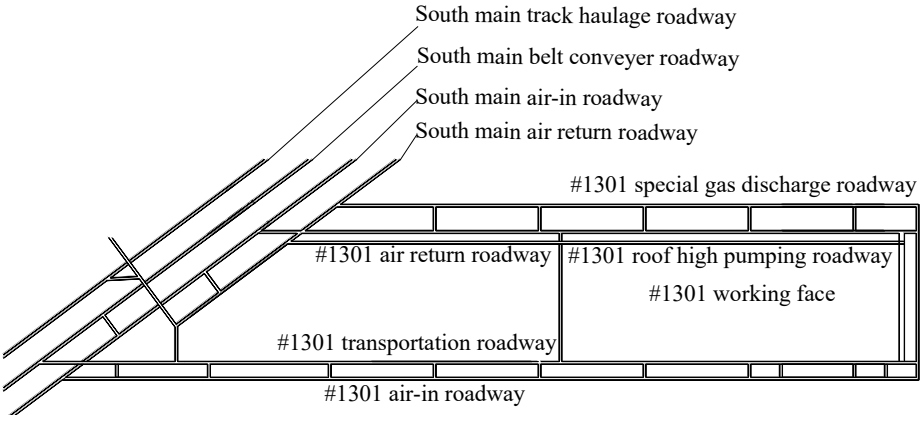

(a) Excavation plan of #1301 working face.

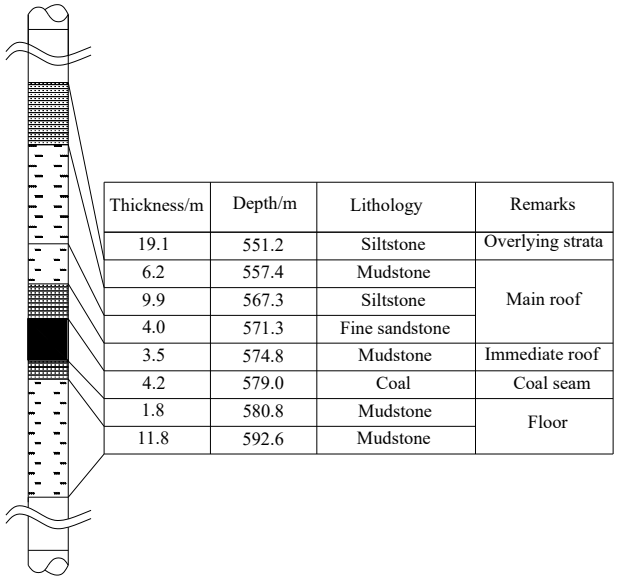

Thickness/m	Depth/m	Lithology	Remarks
19.1	551.2	Siltstone	Overlying strata
6.2	557.4	Mudstone	Main roof
9.9	567.3	Siltstone	
4.0	571.3	Fine sandstone	
3.5	574.8	Mudstone	Immediate roof
4.2	579.0	Coal	Coal seam
1.8	580.8	Mudstone	Floor
11.8	592.6	Mudstone	

(b) Comprehensive column chart of coal seam and roof and floor of #1301 working face.

Fig. 9 General mining and geology conditions of #1301 working face in Licun Coal Mine.

The section of the #1301 transportation roadway is a rectangular section with width × height = 5.5 m × 4.0 m. The roadway is driven along the roof of the coal seam and supported by bolts, metal meshes, and anchor cables. The width of coal pillars in the section is 25 m. The roof of #1301 transportation roadway consists of seven Φ22mm × L2.4m screw thread steel bolts with a row spacing of 0.8m × 0.9m; the row spacing of anchor cables at the roof is 2.0 m × 1.8 m, the length of anchor cables is 7.3 m. The anchor cables are arranged symmetrically along the center line of the roadway. Two ribs are supported by Φ22mm × L2.4m high-strength deformed steel bolts with a row spacing of 0.9 m × 0.9 m.

In order to further meet the needs of mining replacement and gas treatment, and improve the recovery rate of high-quality coal, the #1301 transportation roadway is retained as the mining roadway of #1303 working face. The end hydraulic support of #1301 working face is ZY13000/28/62D, the length of the top beam of the hydraulic support is 5.5 m, and the support strength is 1.1 MPa. The periodic weighting length of the main roof is 20 m, the immediate roof thickness is 3.5 m, the tensile strength is 1.5 MPa, the compressive strength is 12.8-33.6 MPa, and the cutting depth of the coal cutter is 0.8 m.

The roadside filling body #1301 transport roadway is constructed with high water quick-setting materials and water-cement ratio of 1.5:1, with a width of 2.5 m. The minimum pedestrian width behind the end hydraulic support is 0.8 m. Two rows of Φ18.9 mm × L7.3 m anchor cables are added in the middle of the two rows of roadway roof

anchor cables, and the row spacing is 2.0 m × 1.8 m. Two rows of Φ18.9 mm × L4.3 m anchor cables are added in the middle of the two rows of roadway solid coal rib bolts, and the row spacing is 1.5 m × 0.9 m. The single hydraulic prop and type steel beam are used to reinforce the retained roadway within the 100 m range behind the working face, and the column row spacing is 1.0 m×1.0 m. In order to prevent roof falling and layer separation above the roadside filling area, polyester fiber mesh is laid in front of 5 hydraulic supports in the end area. At the same time, a row of Φ22 mm × L2.4 m bolts are installed with a row spacing of 0.8 m × 0.8 m. Φ18.9 mm × L4.3 m anchor cables are drilled every two rows of bolts behind the end hydraulic support, with a row spacing of 1.5 m × 1.6 m.

5.2.2 Determine the cyclic filling length in GER-RF of #1301 working face

According to the above comprehensive column chart, the overburden thickness can be determined to be 23.6 m (3.5 m+4 m+9.9 m+6.2 m), and the average bulk density is 2.5 t/m^3, the load of the overburden rock layer is 0.59 MPa. According to the above, L_1= 10 m, L_2 = 5.5 m, L_3+ L_4= 20 m. By substituting the above data into the calculation, the immediate roof horizontal stress distribution cloud map of the retained roadway with different lengths of the lagging unsupported roof is obtained, as shown in Fig. 10.

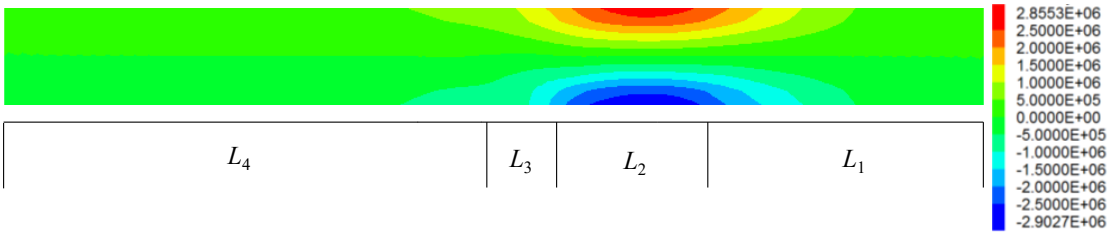

(a) Length of the lagging unsupported roof is 2.5 m.

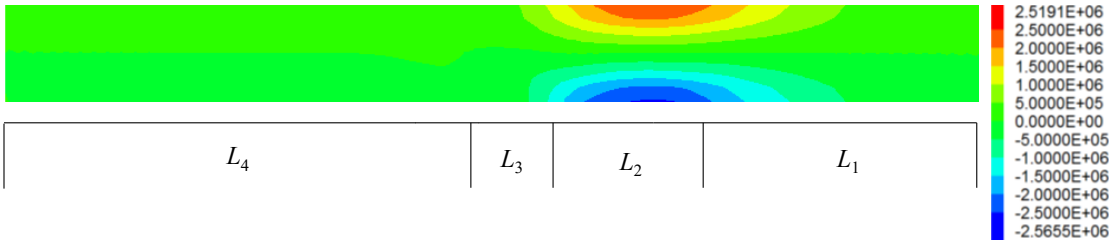

(b) Length of the lagging unsupported roof is 3.0 m.

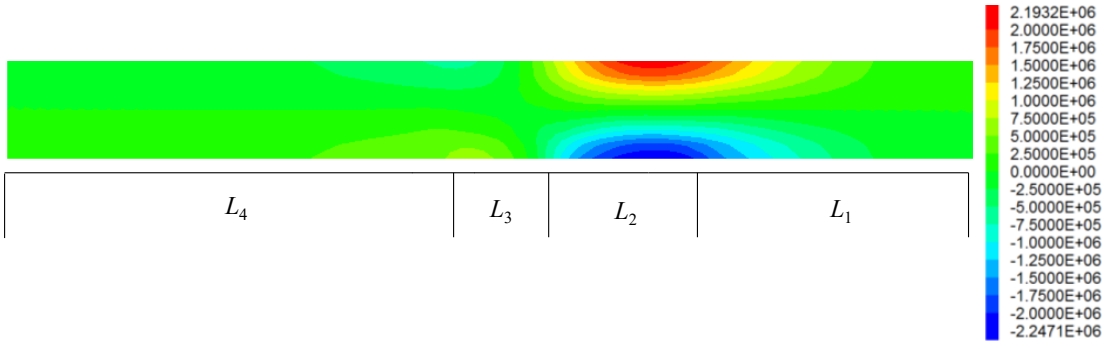

(c) Length of the lagging unsupported roof is 3.5 m.

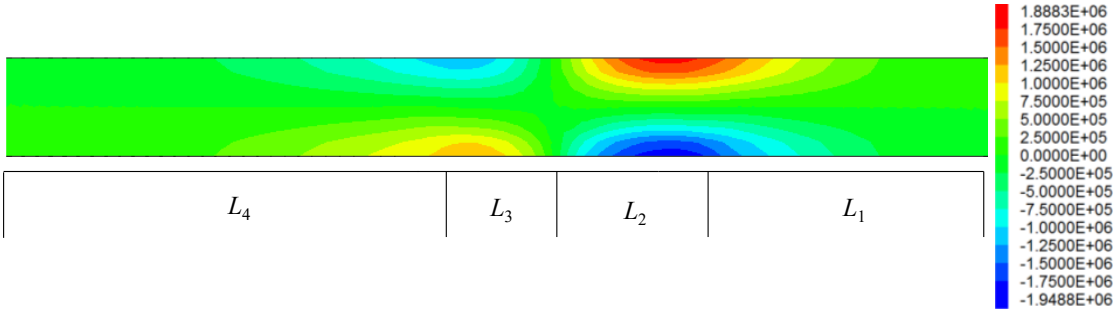

317

318 (d) Length of the lagging unsupported roof is 4.0 m.

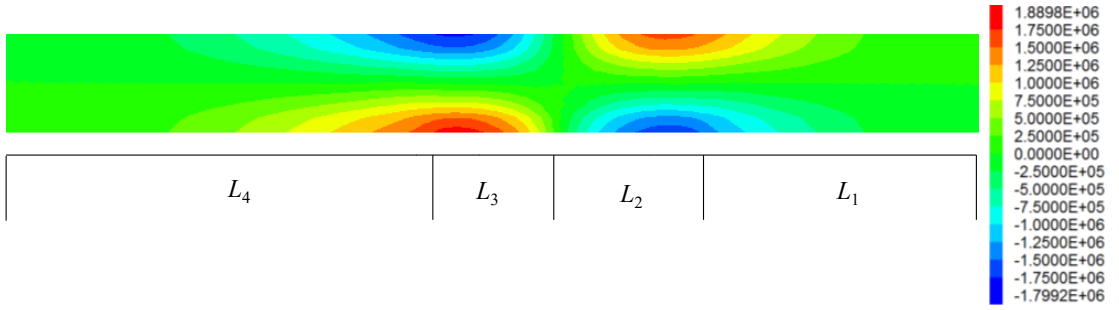

319

320 (e) Length of the lagging unsupported roof is 4.5 m.

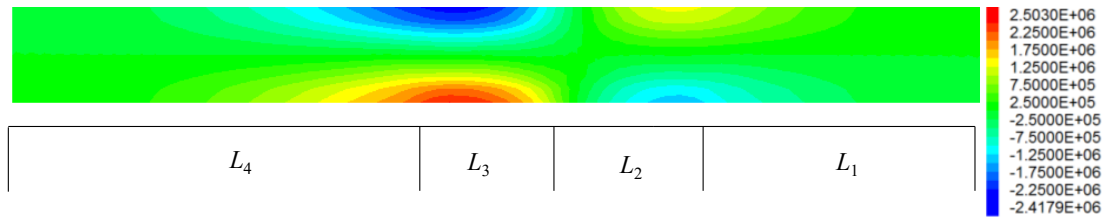

321

322 (f) Length of the lagging unsupported roof is 5.0 m

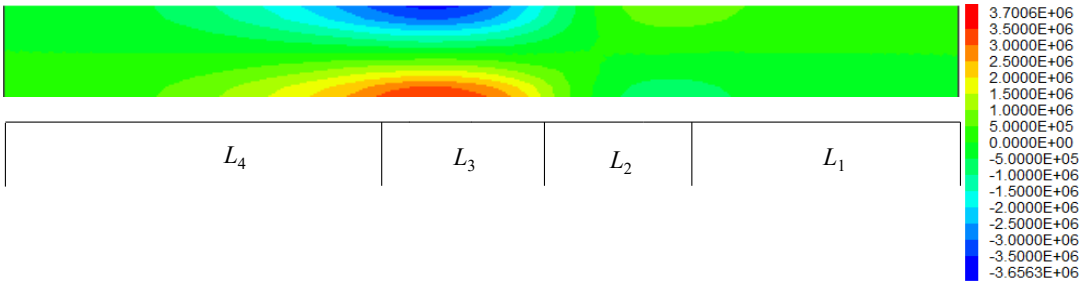

323

324 . (g) Length of the lagging unsupported roof is 6.0 m.

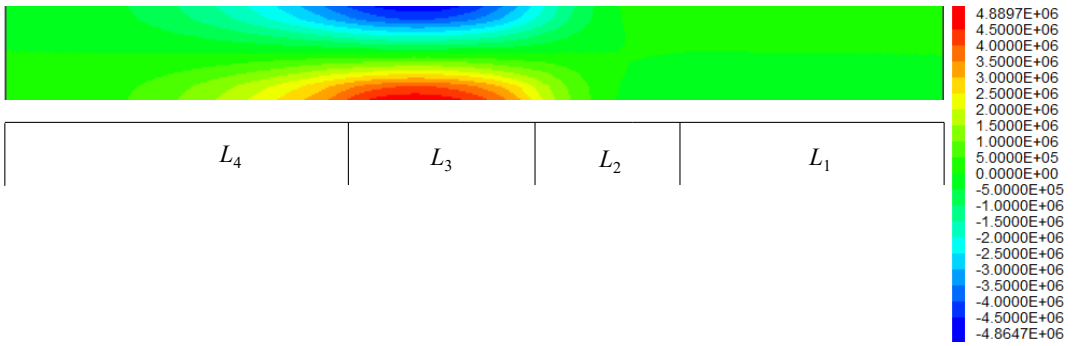

325

326 (h) Length of the lagging unsupported roof is7.0 m.

327 Fig. 10 Immediate roof horizontal stress distribution cloud map of the retained roadway with different lengths of the lagging

unsupported roof. (unit:Pa).

According to Fig. 10, the horizontal stress distribution of the immediate roof of the retained roadway with different length of the lagging unsupported roof is as follows:

1) When the length of the lagging unsupported roof is no more than 3.0 m, the upper immediate roof rock is subjected to the tensile stress, while the lower immediate roof rock is subjected to the compressive stress. The maximum compressive stress occurs in the middle of the immediate roof bottom boundary of the end hydraulic support section and the maximum tensile stress occurs in the middle of the immediate roof boundary of the end hydraulic support section.

2) When the length of the lagging unsupported roof is greater than 3.0 m and less than 7.0 m, the upper immediate roof rock above the unsupported area is subjected to compressive stress, and the lower immediate roof rock above the unsupported area is subjected to tensile stress. The upper immediate roof rock above end hydraulic support is subjected to compressive stress, and the lower immediate roof rock above end hydraulic support is subjected to tensile stress.

3) When the length of the lagging unsupported roof is greater than 7.0 m, the upper immediate roof rock is subjected to compressive stress, and the lower immediate roof rock is subjected to tensile stress. The maximum tensile stress occurs in the middle of the lower boundary above the unsupported area and the maximum compressive stress occurs in the middle of the upper boundary above the unsupported area.

With the increase of the length of the lagging unsupported roof, the maximum tensile stress at the lower part of the immediate roof above the unsupported area gradually increases, and the detailed results are shown in Table 2.

Table 2 Maximum tensile stress of the lower immediate roof in GER-RF with respect to the length of the lagging unsupported roof and cyclic filling length.

Length of the lagging unsupported roof /m	Cyclic filling length/m	Maximum tensile stress /MPa
2.5	1.7	-0.72
3.0	2.2	-0.03
3.5	2.7	0.59
4.0	3.2	1.25
4.5	3.7	1.87
5.0	4.2	2.503
5.5	4.7	3.114
6.0	5.2	3.7
6.5	5.7	4.2993
7.0	6.2	4.8897

According to the aforementioned immediate roof tensile strength of 1.5 MPa, when the length of the lagging unsupported roof is no less than 4.5 m (cyclic filling length is no less than 3.7 m), the lower immediate roof rock above the roadside filling area is subjected to the tensile stress. Taking integer times of the coal cutter cutting depth, the rational cyclic filling length is 3.2 m.

5.2.3 Model validation and implementation effect

No caving or other instability failure occurred in the filling area during the implementation of GER-RF. This indicates that the cyclic filling length and the length of the lagging unsupported roof are appropriate and the proposed model is rational. The in-situ monitoring results show that the surrounding rock deformation of the retained roadway tends to be stable 100 m behind the #1301 working face, the maximum displacement of the roof to floor is 710 mm, and the displacement of two ribs is not more than 530 mm.

Fig. 11 shows the implementation effect of GER-RF in Licun Coal Mine. The above monitoring shows that the

surrounding rock of the retained roadway is basically intact after GER-RF, which meets the expected requirements, and the cyclic filling length of the roadside filling body determined by the study meets the requirements for ensuring safe construction of GER-RF.

Fig. 11 GER implementation effect of #1301 working face in Licun Coal Mine

6 Discussion

In reality, GER-RF support includes road-in support and roadside support. The determination of the cyclic filling length in GER-RF belongs to roadside support problems. At present, there are no published reports at home and abroad on the determination method and theory of the cyclic filling length in GER-RF. Consequently, a theoretical calculation method to determine the cyclic filling length of GER-RF is firstly provided in this paper. According to the theoretical calculation method, the main influence factors to determine the cyclic filling length of GER-RF include the immediate roof tensile strength, roadside filling body strength, support strength of the end hydraulic support and production rates.

6.1 Relationship between the immediate roof tensile strength and the rational cyclic filling length of GER-RF

For Heilong Coal Mine, according to the calculated results shown in Table.2, the relationship between the immediate roof tensile strength and the rational cyclic filling length of GER-RF is shown in Fig.12a. For Licun Coal Mine, according to the calculated results shown in Table.2, the relationship between the immediate roof tensile strength and the rational cyclic filling length of GER-RF is shown in Fig.12b.

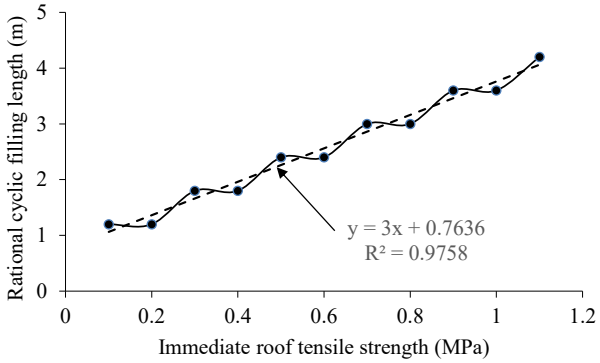

(a) Heilong Coal Mine

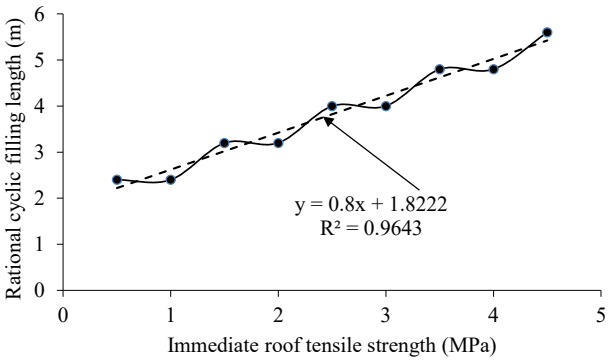

(b) Licun Coal Mine

Fig. 12 Relationship between the immediate roof tensile strength and the rational cyclic filling length

As the immediate roof tensile strength increases, the rational cyclic filling length increases. When the immediate roof tensile strength increases, tensile failure is more difficult to occur in the immediate roof above the filling area. In addition, the immediate roof maintains integrity before the end hydraulic support moves forward, the rational cyclic filling length would be greater, and the GER-RF operational efficiency would be higher.

6.2 Relationship between the roadside filling body strength, the support strength of the end hydraulic support and the cyclic filling length of GER-RF

Consequently, with the increase of the roadside filling body strength, the tensile failure is more difficult to occur in the immediate roof above the filling area. Research results have shown that the greater the roadside filling body strength, the fewer the main roof rotation angle and the less tensile stress action range above the filling area (Zhang et al. 2018). Moreover, the relationship between the support strength of the end hydraulic support and the cyclic filling length of GER-RF presents the same pattern.

6.3 Relationship between the production rates and the cyclic filling length of GER-RF

In reality, during the implementation of GER-RF, the rational daily cyclic filling length is greater than the daily working face mining length (production rates). In order to match the daily mining length of high-efficiency fully mechanized mining working face, the rational cyclic filling length is adjust to the daily production plan and the daily cutting depth of the coal cutter.

7 Conclusion

The construction of the roadside filling body is the key to match the GER-RF speed with the mining speed of the high-efficiency fully mechanized working face. How to determine the rational cycle filling length of roadside filling body not only affects consumption of building and removing the formwork of the roadside filling body but also affects the mining process of the fully mechanized working face. At present, there is no theoretical approach to determine cyclic filling length in GER-RF. In this paper, we establish a plane strain calculation model between the immediate roof and the below support elements based on the GER-RF surrounding rock structure and stress characteristics. Then, a detailed stress difference method is proposed to calculate the stress analytic value of the immediate roof. Finally, according to the relationship between the tensile stress of the immediate roof and its ultimate tensile strength, the rational cyclic fill length of the roadside filling body in GER-RF is obtained. The main conclusions include:

1) The relationship between the distribution of tensile stress in different areas of GER-RF and the length of the lagging unsupported roof are obtained by using the stress difference method to solve the immediate roof stress of GER-RF. Then, the stability of the immediate roof in the area to be filled are determined by comparing the immediate roof stress with the ultimate tensile strength, and the safe length of the lagging unsupported roof and the reasonable cyclic filling length are obtained.

2) Engineering trial tests carried out in different thickness coal seam (thin coal seam of Heilong Coal Mine and thick coal seam of Licun Coal Mine) indicate that the proposed method to determine the cyclic filling length is rational and validated. This research is beneficial for developing a practical approach to obtain the cyclic filling length in GER-RF, and also provides a practical approach to determine the unsupported roof length in the roadway drivage.

Availability of data and materials

The datasets used or analyzed during the current study are available from the corresponding author on reasonable request.

Competing interests

The authors have declared that no competing interests exist.

Authors' contributions

Zizheng Zhang, Jianbiao Bai, Weijian Yu contributed to the conception of the study; Xianyang Yu, Min Deng, Jinlin Xin contributed significantly to analysis and manuscript preparation; Zizheng Zhang performed the data analyses and wrote the manuscript; Xianyang Yu helped perform the analysis with constructive discussions.

Acknowledgements

The project was supported by the National Natural Science Foundation of China through Contract (No. 51804111, 51774133, 51904102), and Natural Science Foundation of Hunan Provincial (No. 2020JJ5194).

References

Kang HP, Niu DL, Zhang Z, Lin J, Li ZH, Fan MJ (2010) Deformation characteristics of surrounding rock and supporting technology of gob-side entry retaining in deep coal mine. Chinese Journal of Rock Mechanics and Engineering 29: 1977-1987.

Han CL, Zhang N, Xue JH, Kan JG, Zhao YM (2019) Multiple and long-term disturbance of gob-side entry retaining by grouped roof collapse and an innovative adaptive technology. Rock Mech. Rock Eng 52: 2761-2773.

Zhang ZZ, Bai JB, Chen Y, Yan S (2015) An innovative approach for gob-side entry retaining in highly gassy fully-mechanized longwall top-coal caving. Int. J. Rock Mech. Min. Sci 80: 1-11.

Yang HY, Liu YB, Cao SG, Pan RK, Wang H, Li Y, Luo F (2020) A caving self-stabilization bearing structure of advancing cutting roof for gob-side entry retaining with hard roof stratum. Geomech. Eng 21: 23-33.

Ning JG, Liu XS, Tan J, Gu QH, Tan YL, Wang J (2018) Control mechanisms and design for a "coal-backfill-gangue" support system for coal mine gob-side entry retaining. Int. J. Oil Gas Coal Tech 18: 444-466.

Zhang ZZ, Wang WJ, Li SQ, Yu XY (2018) An innovative approach for gob-side entry retaining with thick and hard roof: A case study. Tech. Gaz 25: 1028-1036.

Luan HJ, Jiang YJ, Lin HL, Li GF (2018) Development of a new gob-side entry-retaining approach and its application. Sustainability 10: 470.

Tian ZJ, Zhang ZZ, Deng M, Yan S, Bai JB (2020) Gob-side entry retained with soft roof, floor, and seam in thin coal seams: a case study. Sustainability 12: 1197.

Wang Q, He MC, Yang J, Gao HK, Jiang B, Yu HC (2018) Study of a no-pillar mining technique with automatically formed gob-side entry retaining for longwall mining in coal mines. Int. J. Rock Mech. Min. Sci 110: 1-8.

Huang WP, Gao YF, Wen ZJ, Gao L (2015) Technology of gob-side entry retaining using concrete-filled steel tubular column as roadside supporting. J. Chin Univ. Min. Tech 44: 604-611.

Su H, Bai JB, Yan S, Chen Y, Zhang ZZ (2015) Study on gob-side entry retaining in fully-mechanized longwall with top-coal caving and its application. Int. J. Min. Sci. Tech 25: 503-510.

Zhang ZZ, Yu XY, Wu H, Deng M (2019) Stability control for gob-side entry retained with supercritical retained entry width in thick coal seam longwall mining. Energies 12: 1375.

Zhang ZZ, Deng M, Bai JB, Yu XY, Wu QH, Jiang, LS (2020) Strain energy evolution and conversion under triaxial unloading confining pressure tests due to gob-side entry retained. Int. J. Rock Mech. Min. Sci 126: 104184.

Zhang ZZ, Bai JB, Wang W, Chen Y, Yu XY (2018) Mechanical analysis of roof separation within and outside anchorage zone above backfill area of gob-side entry retaining and its engineering application. Journal of China Coal Society 35: 893-901.

Zhang ZZ, Deng M, Wang X, Yu WJ, Zhang F, Dao V (2020) Field and numerical investigations on the lower coal seam entry failure analysis under the remnant pillar. Engineering Failure Analysis 115: 104638.

Zheng X, Bai Y (2012) Technology of roof supporting at stowing area in deep roadway retained along gob. Coal Mining Technology 17: 42-45.

Bai JB, Xiao TQ, Li L (2011) Unsupported roof distance determination of roadway excavation using difference method and its application. Journal of China Coal Society 36: 920-924.

Yan S, Wang R, Bai JB, Wu WD, Elmo D (2020) An alternative approach to determine cycle length of roadway excavation in coal mines. J. Ambient Intell. Human Comput 11: 553–560.

Figures

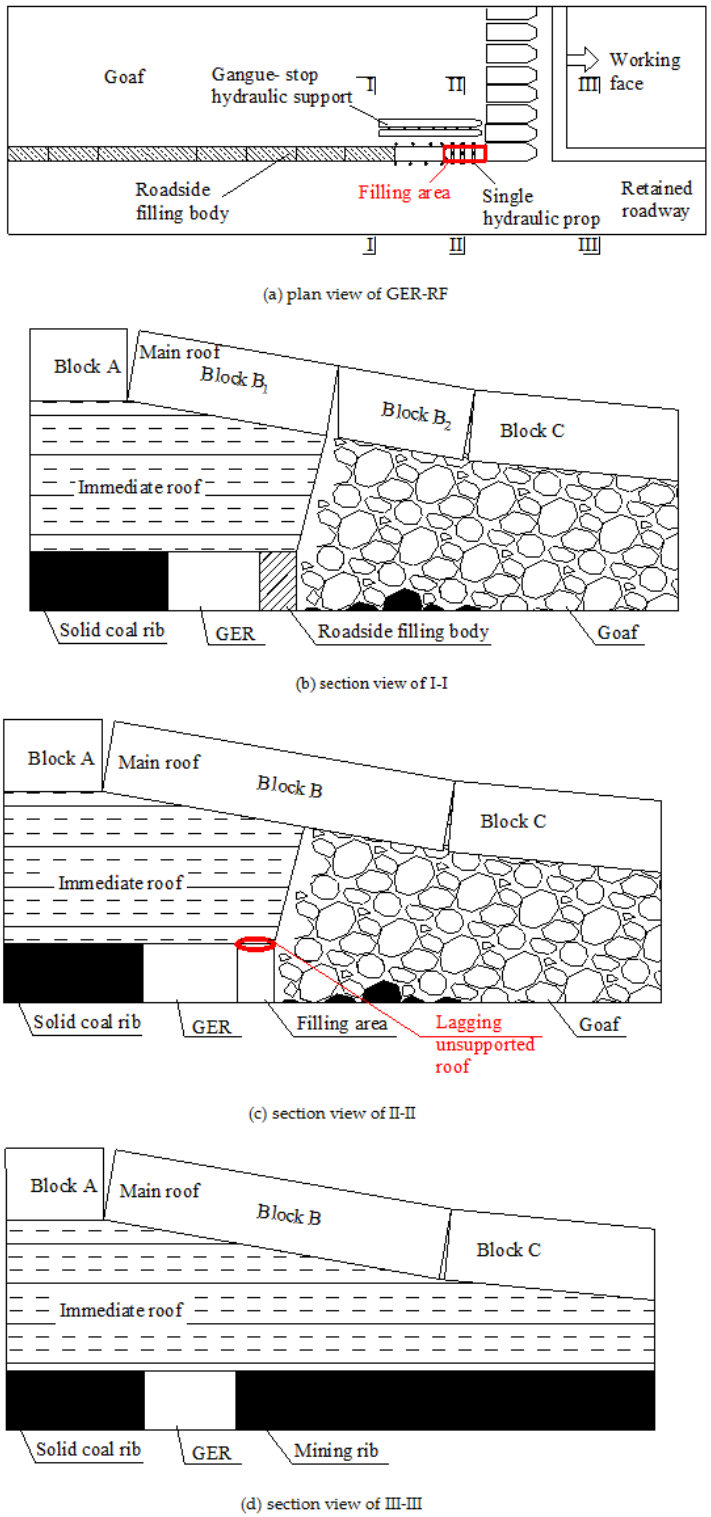

Figure 1

Sketch of lagging unsupported roof in GER-RF

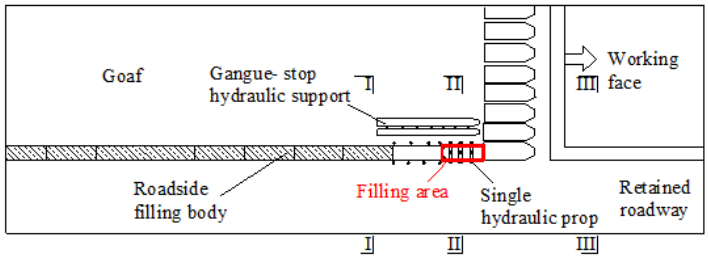

(a) plan view of GER-RF

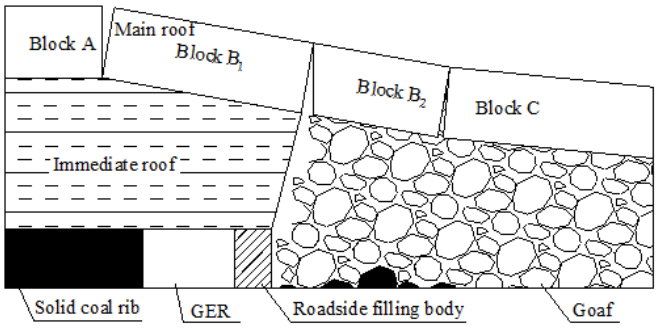

(b) section view of I-I

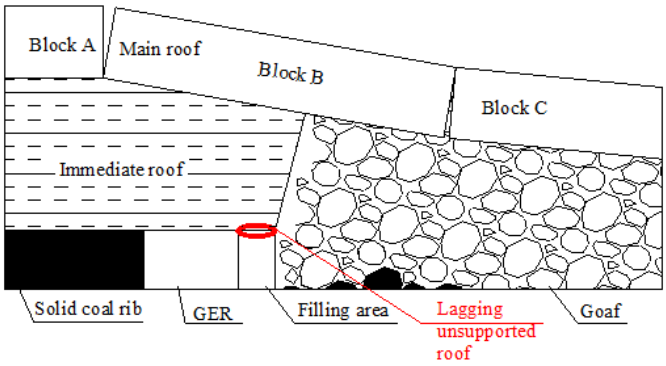

(c) section view of II-II

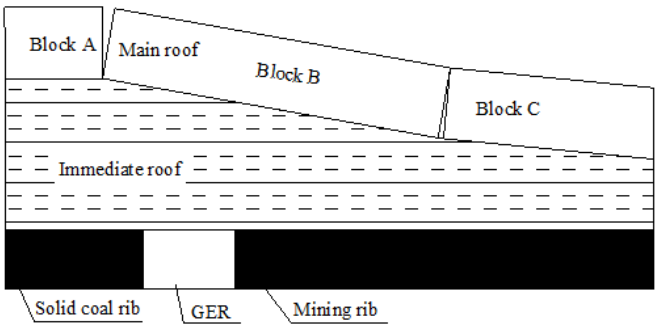

(d) section view of III-III

Figure 1

Sketch of lagging unsupported roof in GER-RF

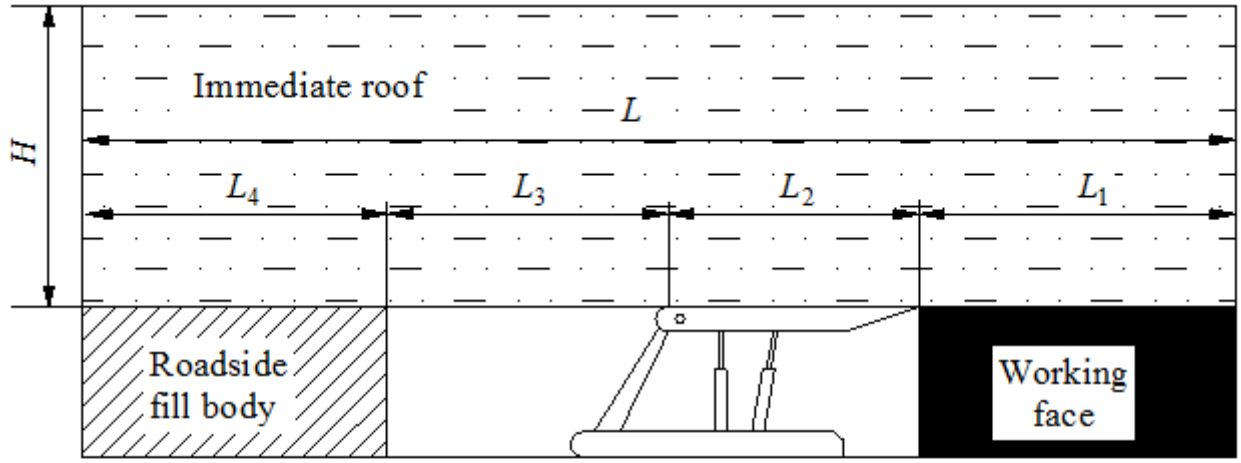

(a) Section of GER-BB along the strike direction.

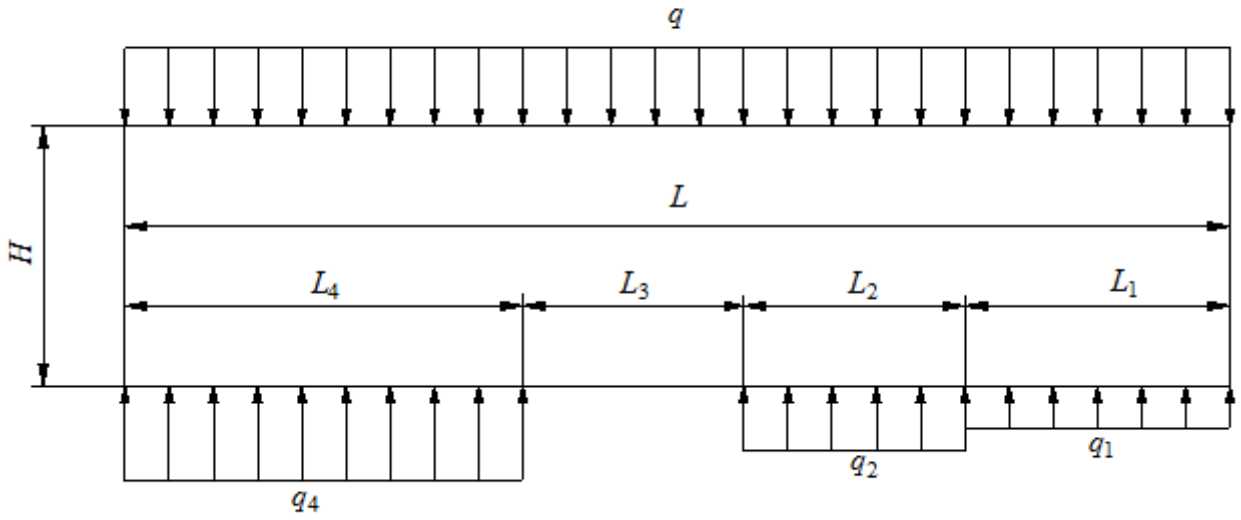

(b) Immediate roof mechanical model in GER-RF along the strike direction.

Figure 2

Mechanical model of immediate roof stability analysis above roadside filling area in GER-RF

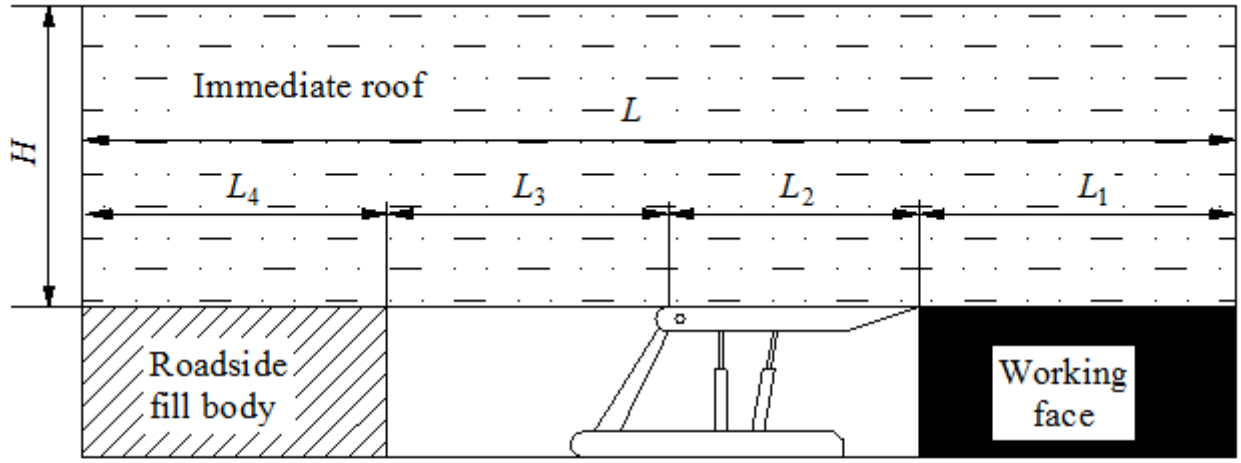

(a) Section of GER-BB along the strike direction.

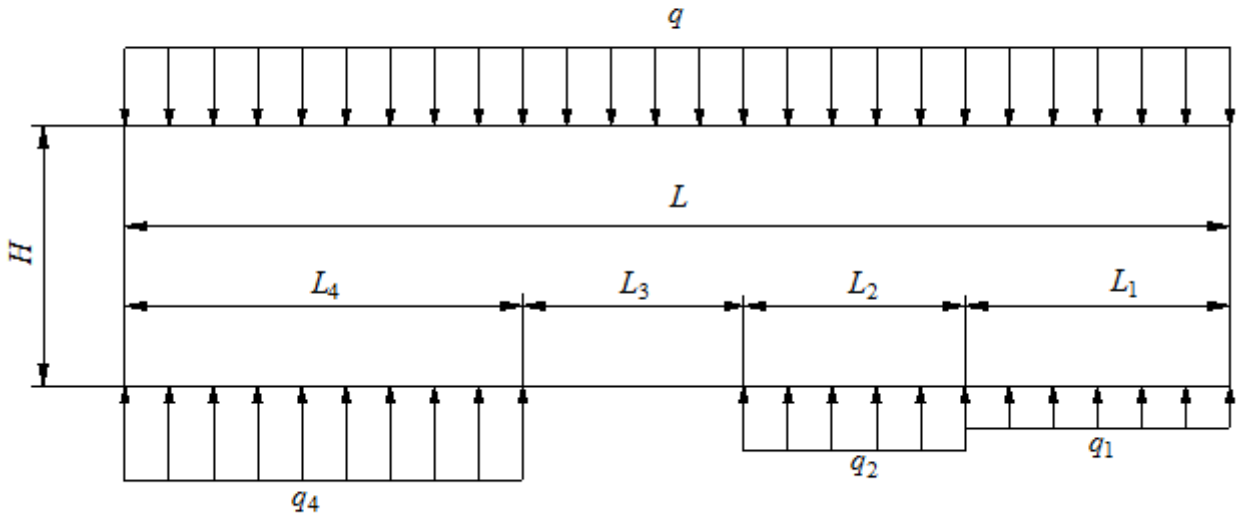

(b) Immediate roof mechanical model in GER-RF along the strike direction.

Figure 2

Mechanical model of immediate roof stability analysis above roadside filling area in GER-RF

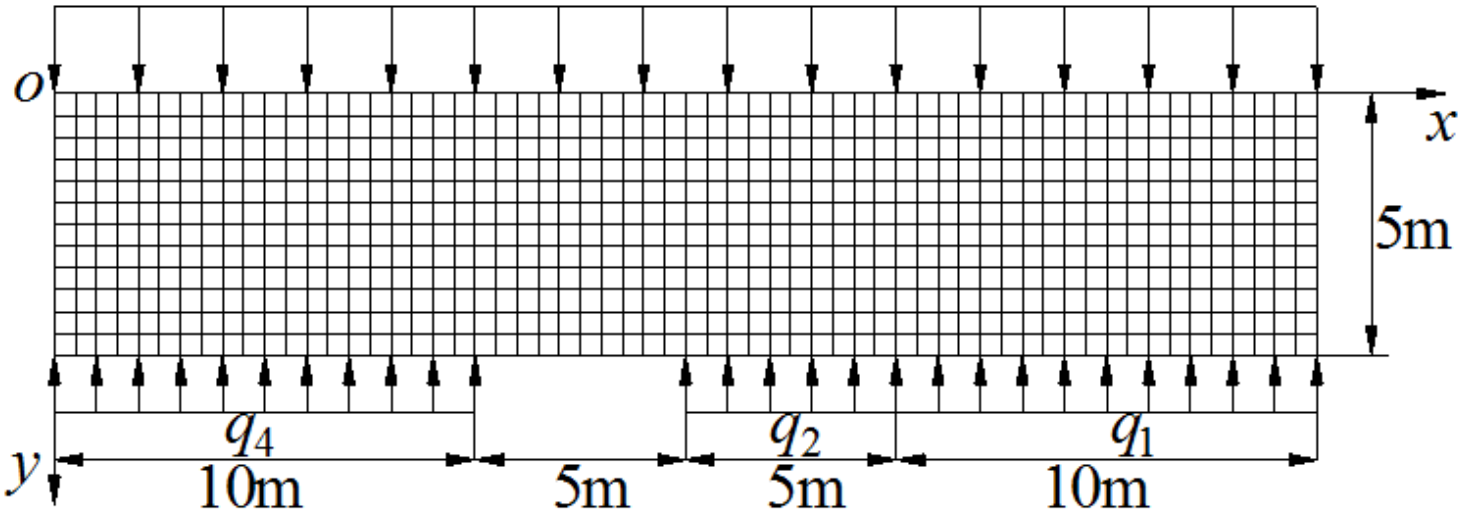

Figure 3

Finite difference elements of the immediate roof in GER-RF

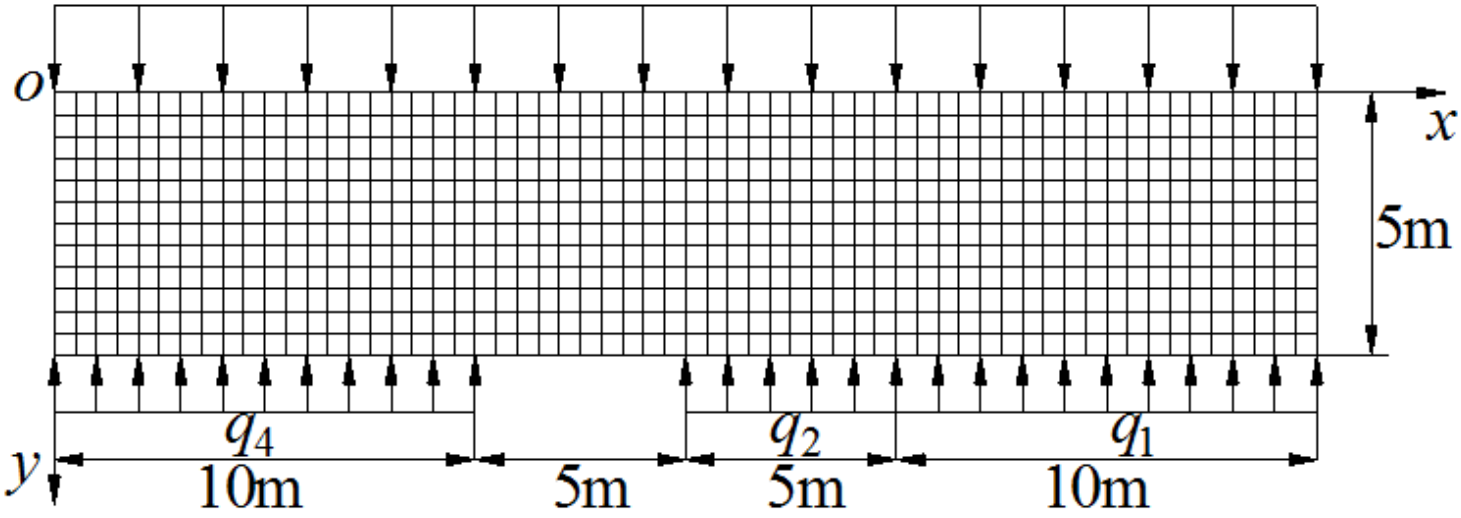

Figure 3

Finite difference elements of the immediate roof in GER-RF

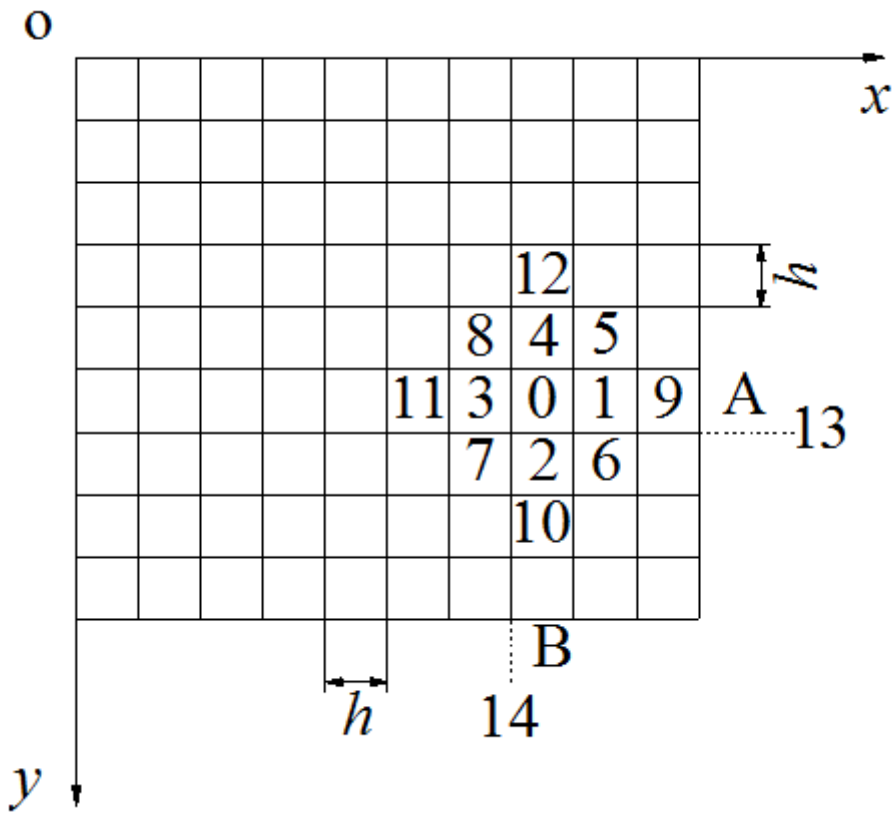

Figure 4

Schematic diagram of the stress difference method

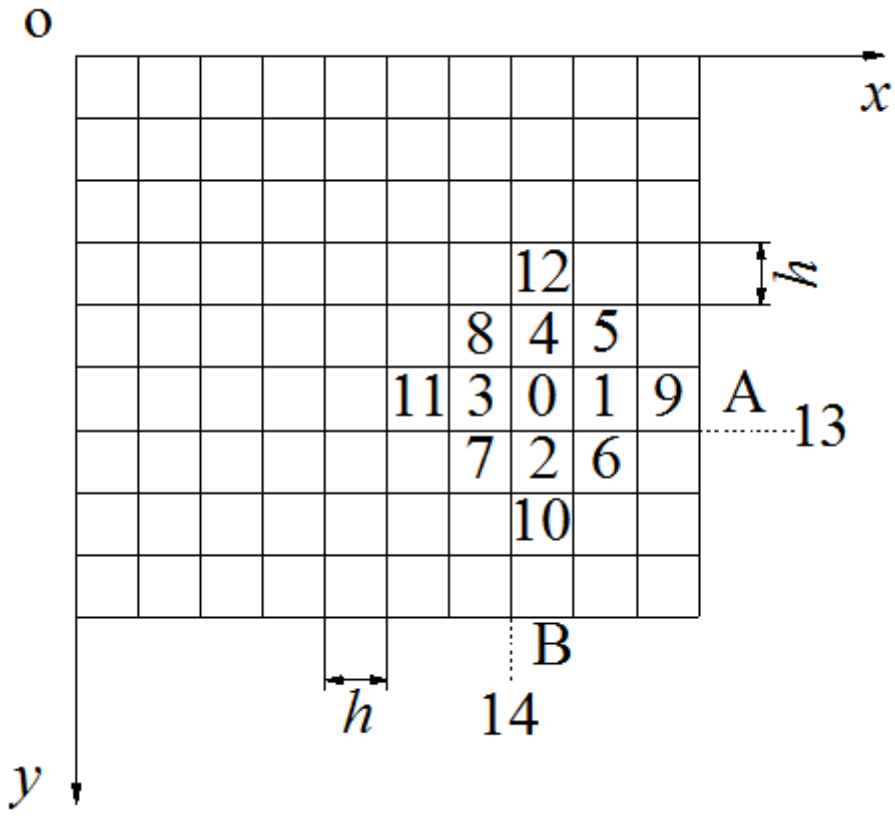

Figure 4

Schematic diagram of the stress difference method

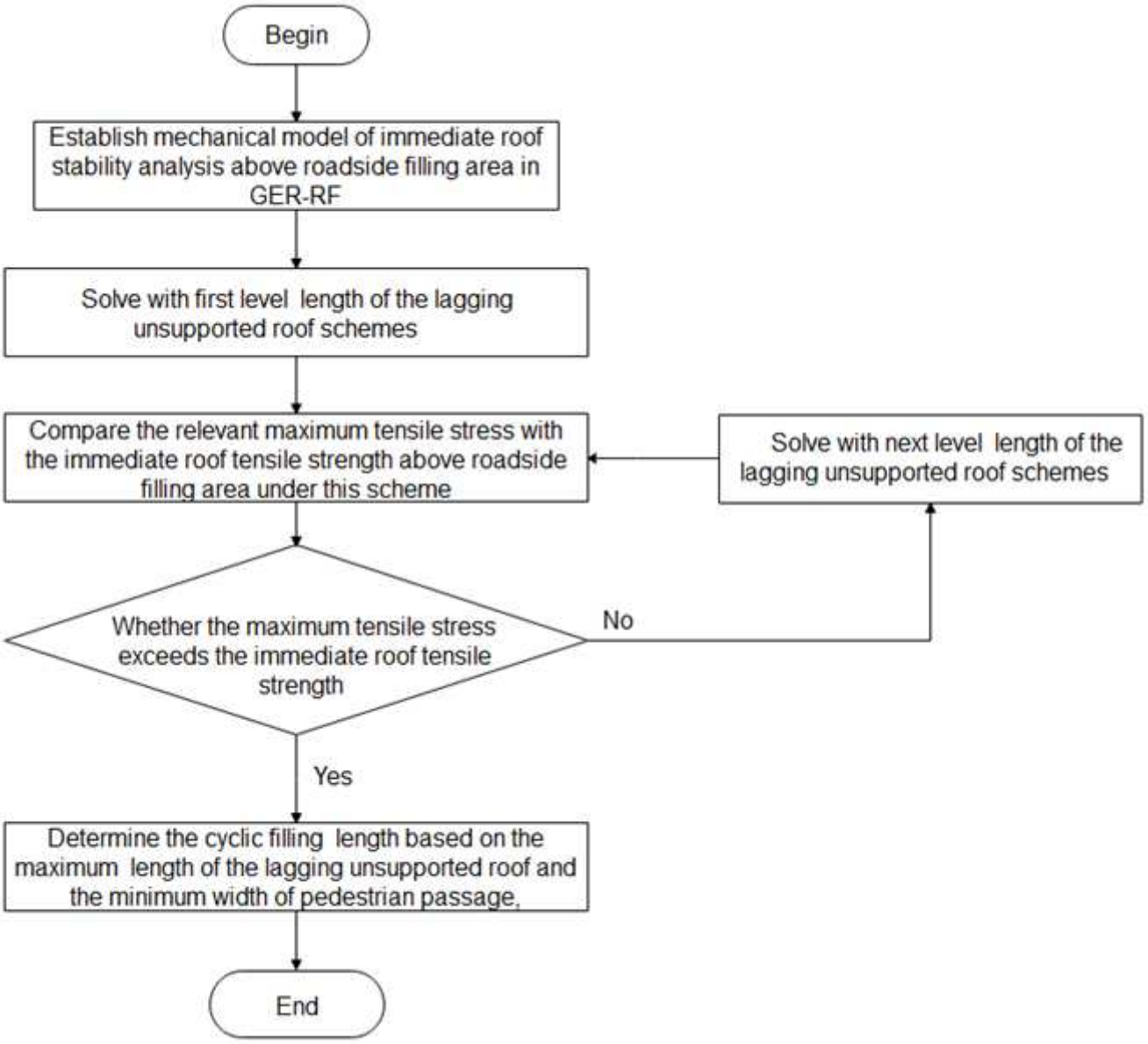

Figure 5

Calculation flow of the cyclic backfill length of GER-BB based on the stress difference method.

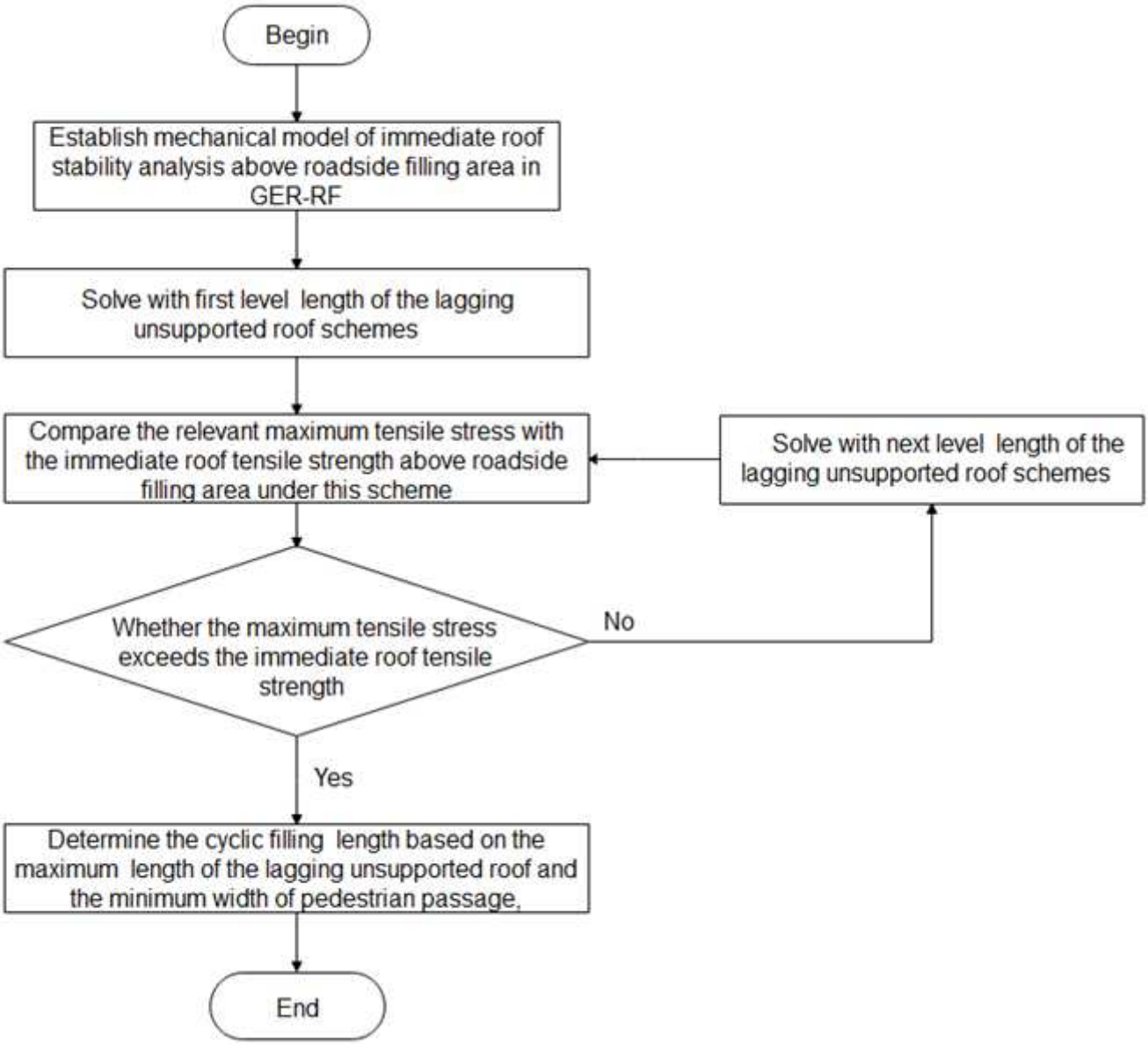

Figure 5

Calculation flow of the cyclic backfill length of GER-BB based on the stress difference method.

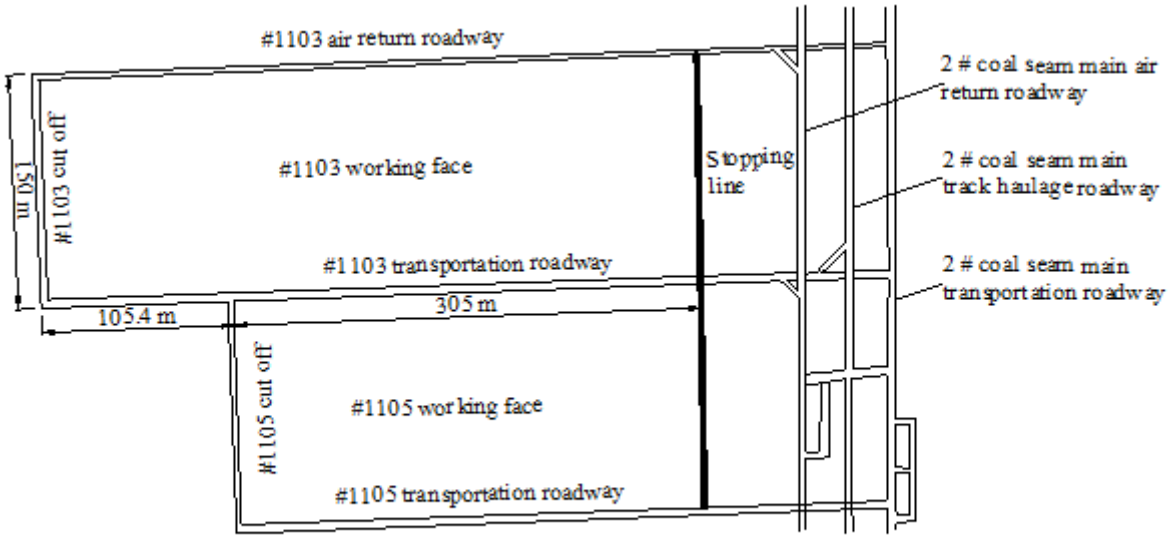

(a) Mining plan of #1103 working face.

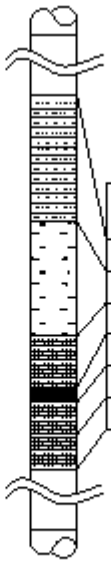

Thickness/m	Depth/m	Lithology	Remarks
11.1	194.2	Sand mudstone	Overlying strata
10.0	204.2	Fine sandstone	Main roof
4.5	208.7	Mudstone	Immediate roof
1.3	210.0	Coal	Coal seam
2.8	212.8	Mudstone	Floor
3.0	215.8	Mudstone	

(b) Comprehensive column chart of coal seam and roof and floor of #1103 working face.

Figure 6

Geological conditions of production at #1103 working face in Heilong Coal Mine.

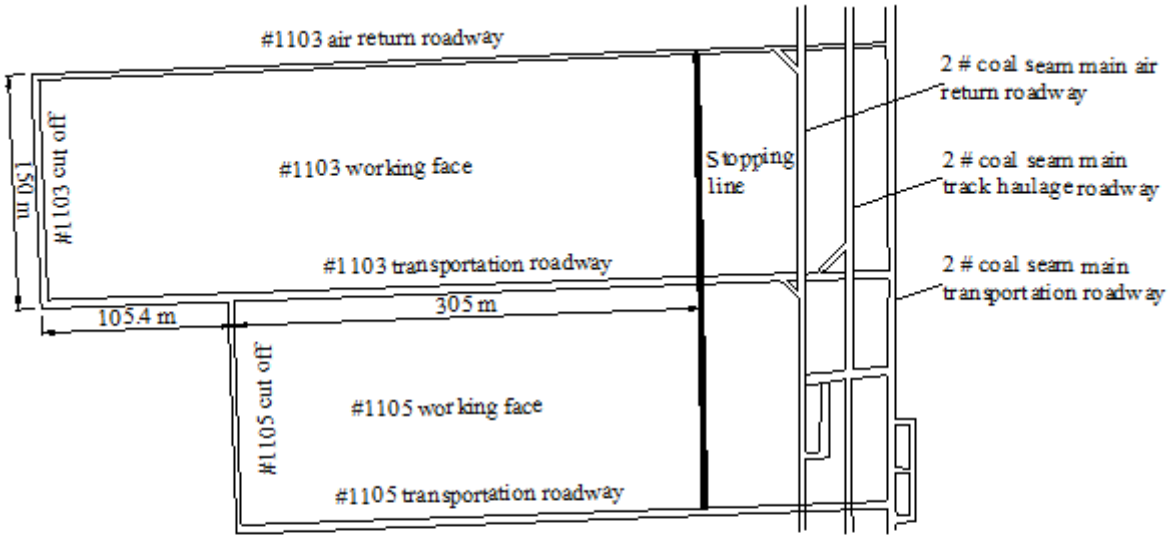

(a) Mining plan of #1103 working face.

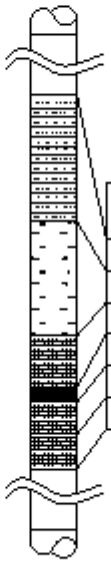

Thickness/m	Depth/m	Lithology	Remarks
11.1	194.2	Sand mudstone	Overlying strata
10.0	204.2	Fine sandstone	Main roof
4.5	208.7	Mudstone	Immediate roof
1.3	210.0	Coal	Coal seam
2.8	212.8	Mudstone	Floor
3.0	215.8	Mudstone	

(b) Comprehensive column chart of coal seam and roof and floor of #1103 working face.

Figure 6

Geological conditions of production at #1103 working face in Heilong Coal Mine.

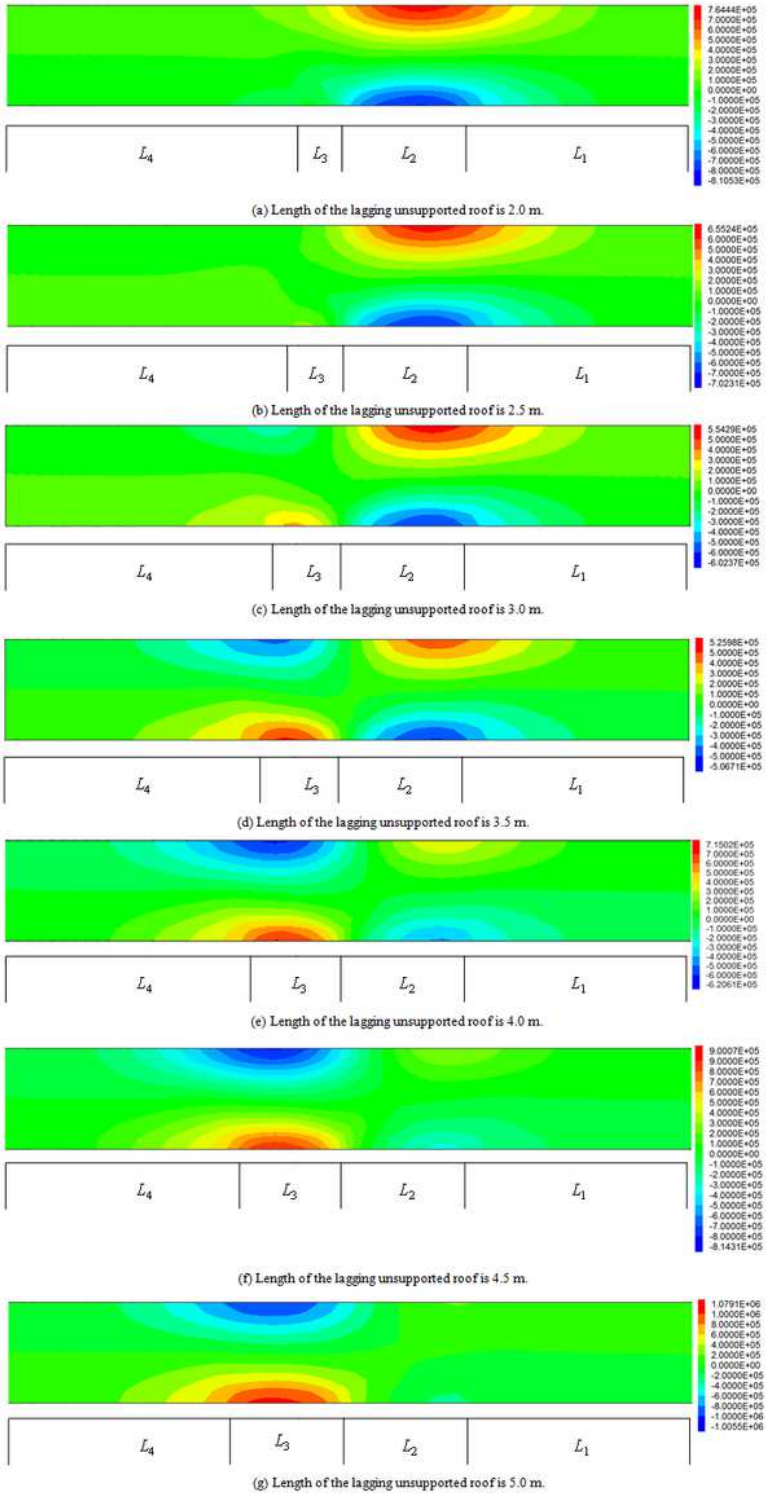

Figure 7

Immediate roof horizontal stress distribution cloud map of the retained roadway with different lengths of the lagging unsupported roof. (unit:Pa).

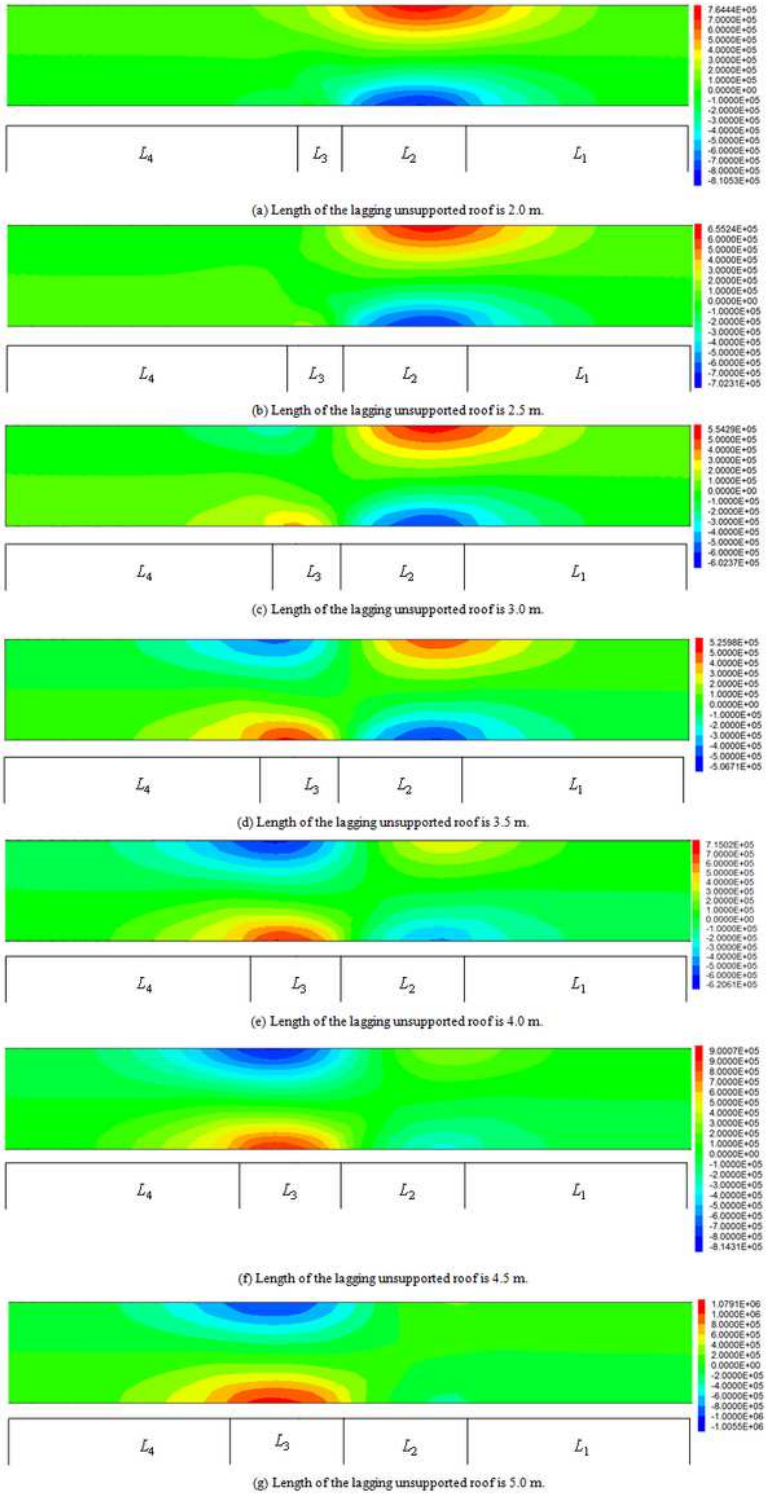

Figure 7

Immediate roof horizontal stress distribution cloud map of the retained roadway with different lengths of the lagging unsupported roof. (unit:Pa).

Figure 8

GER implementation effect of #1103 working face in Heilong Coal Mine

Figure 8

GER implementation effect of #1103 working face in Heilong Coal Mine

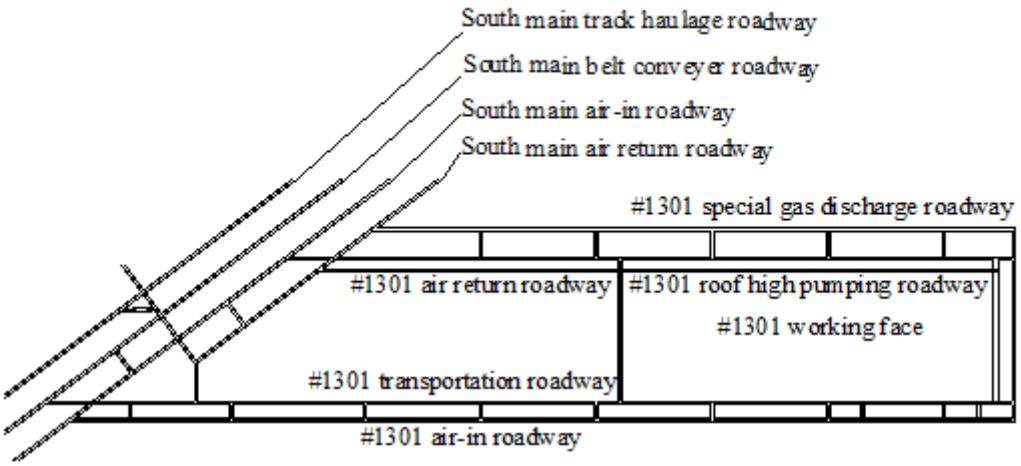

(a) Excavation plan of #1301 working face.

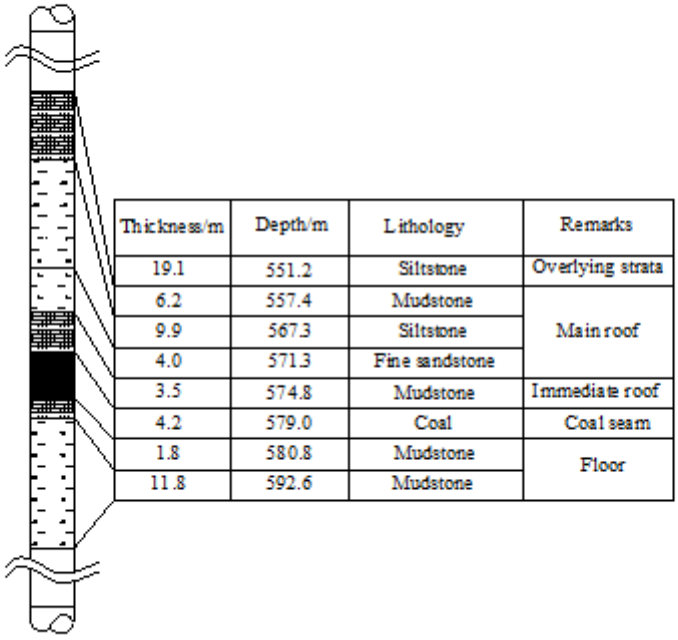

Thickness/m	Depth/m	Lithology	Remarks
19.1	551.2	Siltstone	Overlying strata
6.2	557.4	Mudstone	Main roof
9.9	567.3	Siltstone	
4.0	571.3	Fine sandstone	
3.5	574.8	Mudstone	Immediate roof
4.2	579.0	Coal	Coal seam
1.8	580.8	Mudstone	Floor
11.8	592.6	Mudstone	

(b) Comprehensive column chart of coal seam and roof and floor of #1301 working face.

Figure 9

General mining and geology conditions of #1301 working face in Licun Coal Mine.

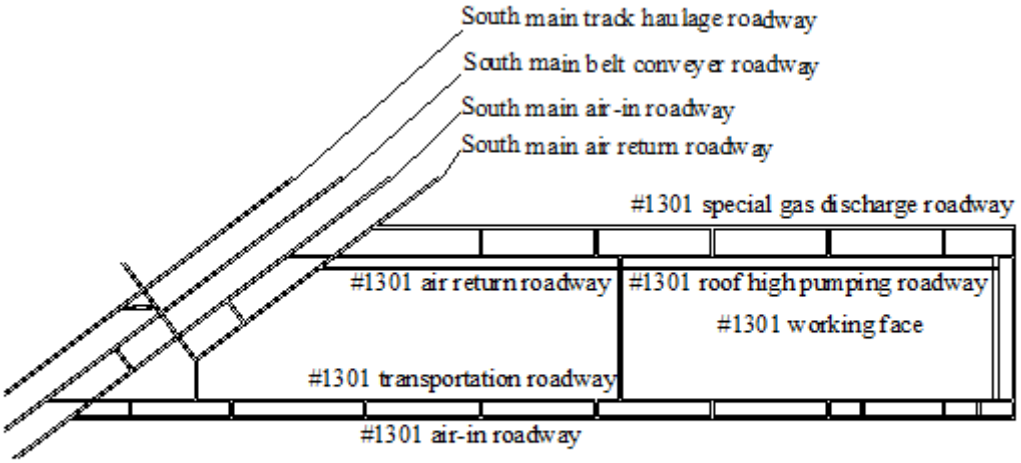

(a) Excavation plan of #1301 working face.

Thickness/m	Depth/m	Lithology	Remarks
19.1	551.2	Siltstone	Overlying strata
6.2	557.4	Mudstone	Main roof
9.9	567.3	Siltstone	
4.0	571.3	Fine sandstone	
3.5	574.8	Mudstone	Immediate roof
4.2	579.0	Coal	Coal seam
1.8	580.8	Mudstone	Floor
11.8	592.6	Mudstone	

(b) Comprehensive column chart of coal seam and roof and floor of #1301 working face.

Figure 9

General mining and geology conditions of #1301 working face in Licun Coal Mine.

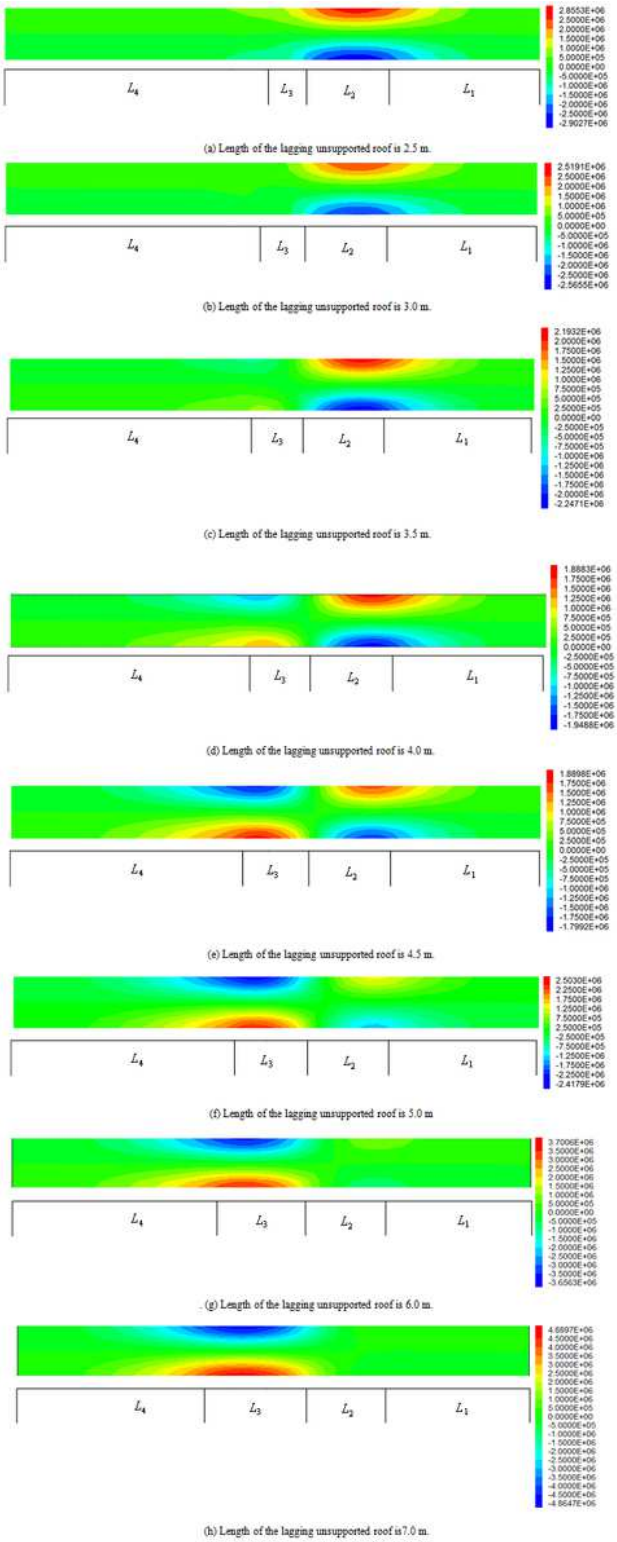

Figure 10

Immediate roof horizontal stress distribution cloud map of the retained roadway with different lengths of the lagging unsupported roof. (unit:Pa).

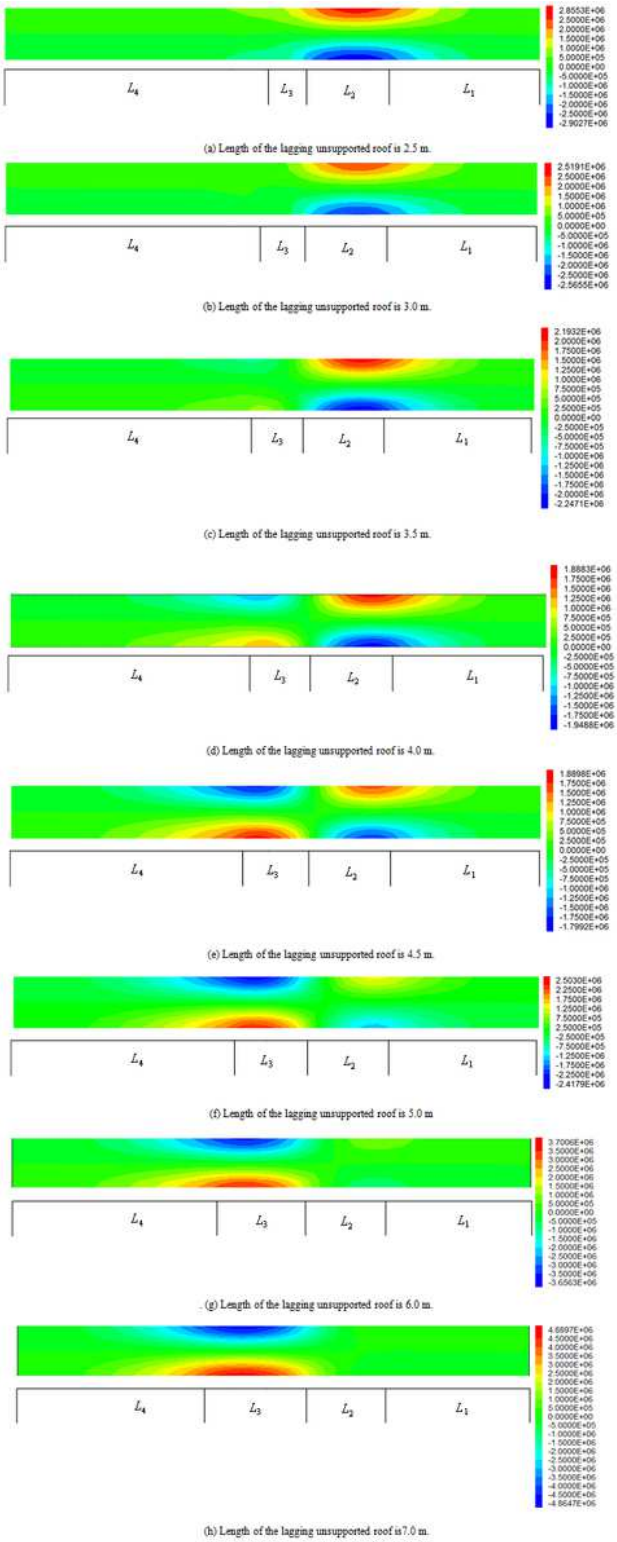

Figure 10

Immediate roof horizontal stress distribution cloud map of the retained roadway with different lengths of the lagging unsupported roof. (unit:Pa).

Figure 11

GER implementation effect of #1301 working face in Licun Coal Mine

Figure 11

GER implementation effect of #1301 working face in Licun Coal Mine

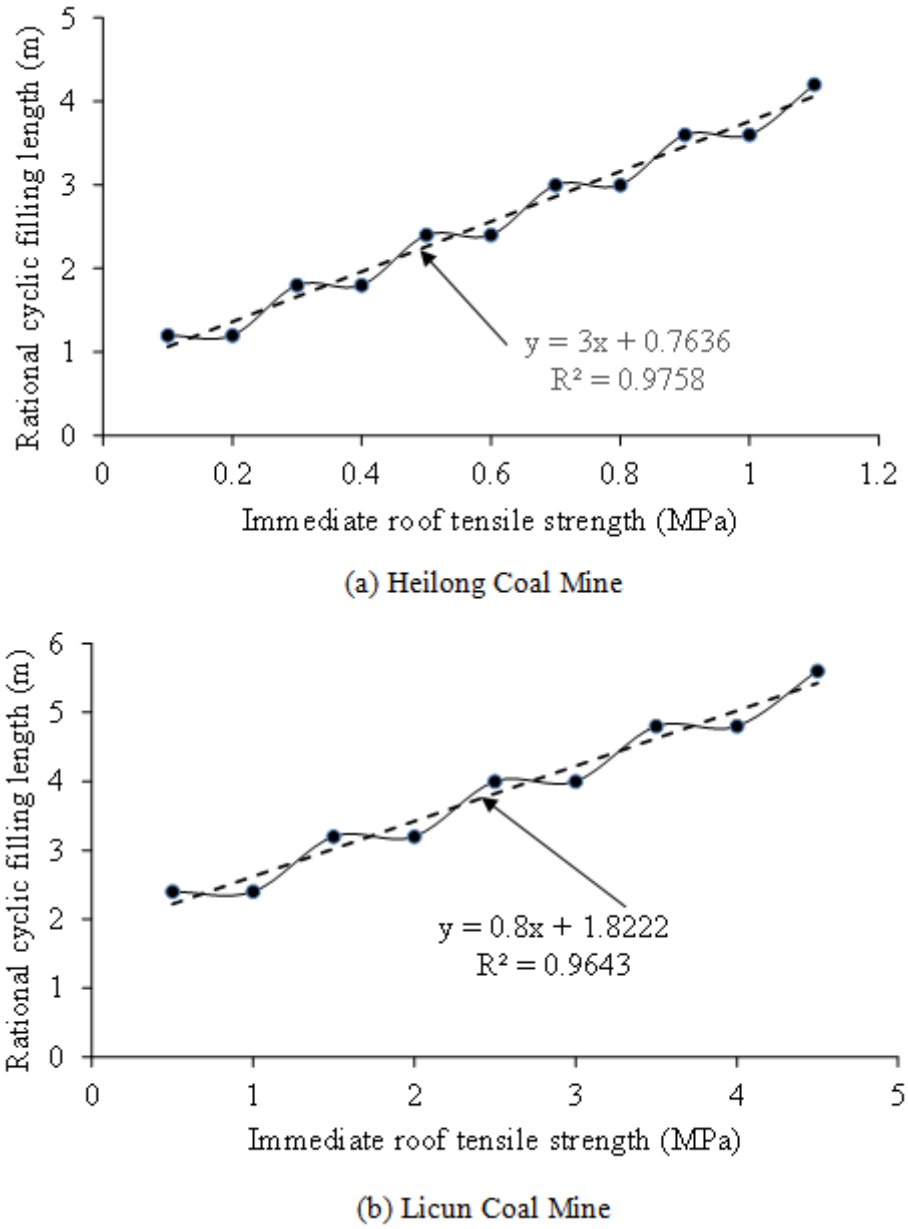

Figure 12

Relationship between the immediate roof tensile strength and the rational cyclic filling length

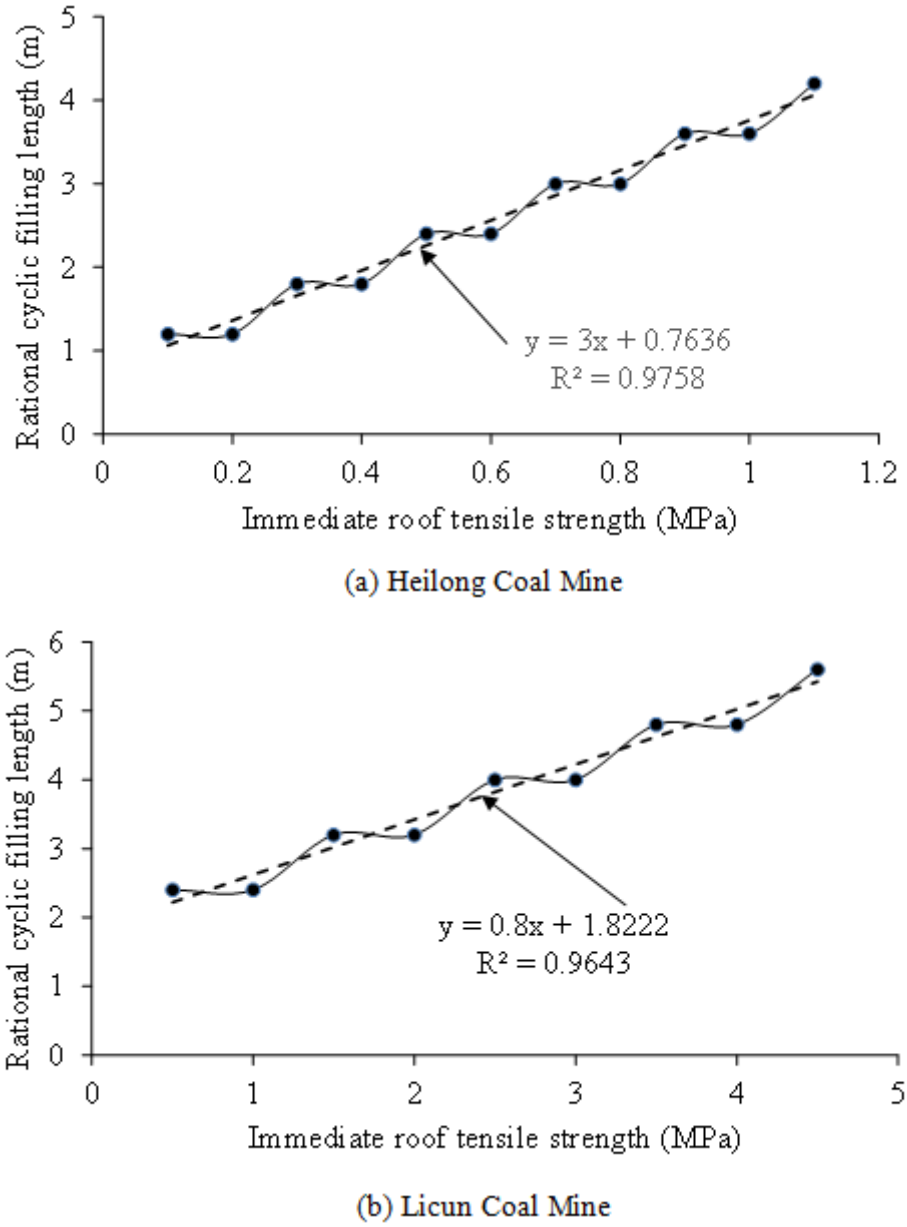

Figure 12

Relationship between the immediate roof tensile strength and the rational cyclic filling length